CHAPTER V

The *in vivo* neuroprotective mechanism of snake venom nerve growth factors-derived custom peptides in *Caenorhabditis elegans*

5.1 Results

5.1.1 *In silico* analysis of custom peptides binding in *C. elegans*

According to the modelling results, mouse NGF 2.5S and custom peptides (TNP and HNP) bind to a CAM-1 receptor domain that resembles the mammalian TrkA receptor and is immunoglobulin (IG)-like. Despite the substantial variations in the total amino acid sequences, the domains of both proteins share a comparable structure. Nonetheless, the amino acid sequences of the binding region of both proteins showed similarities. The tyrosine-protein kinase receptor CAM-1's IG domain was found to be interacting with the custom peptides TNP (Fig 5.1a), HNP (Fig 5.1b), and mouse NGF (Fig 5.1c) exhibited interaction with the IG domain of CAM-1, which is a tyrosine-protein kinase receptor. Nevertheless, the IG domain of the CAM-1 receptor did not show appreciable interaction with scrambled peptide (Fig 5.1d).

The RMSD analysis of the trajectory demonstrated significant stable interaction for all these proteins (Figs 5.1e-h). The MM-GBSA binding free energies obtained for different complexes were between -40 and -51 kcal/mol. The root mean square deviation (RMSD) values exhibited variation up to 4.2 Å.

The custom peptide showed efficient binding with one of the tyrosine-protein kinase receptors CAM-1. Entries in the Reactome pathway browser database [1] suggest that CAM-1 is an essential component in the MAPK signaling pathway by playing multiple roles. Custom peptides TNP (Figs 5.1 A and E), HNP (Figs 5.1B and 5.1F), mouse-NGF (Figs 5.1C and G) form a complex with IG of CAM-1 and exhibited reasonable binding stability. In contrast, scrambled peptide (Figs 5.1D and H) exhibited relatively unstable binding. Notably, BLAST sequence search revealed that CAM-1 shares considerable homology (38.5%) with human NTRKA receptors and functions similarly.

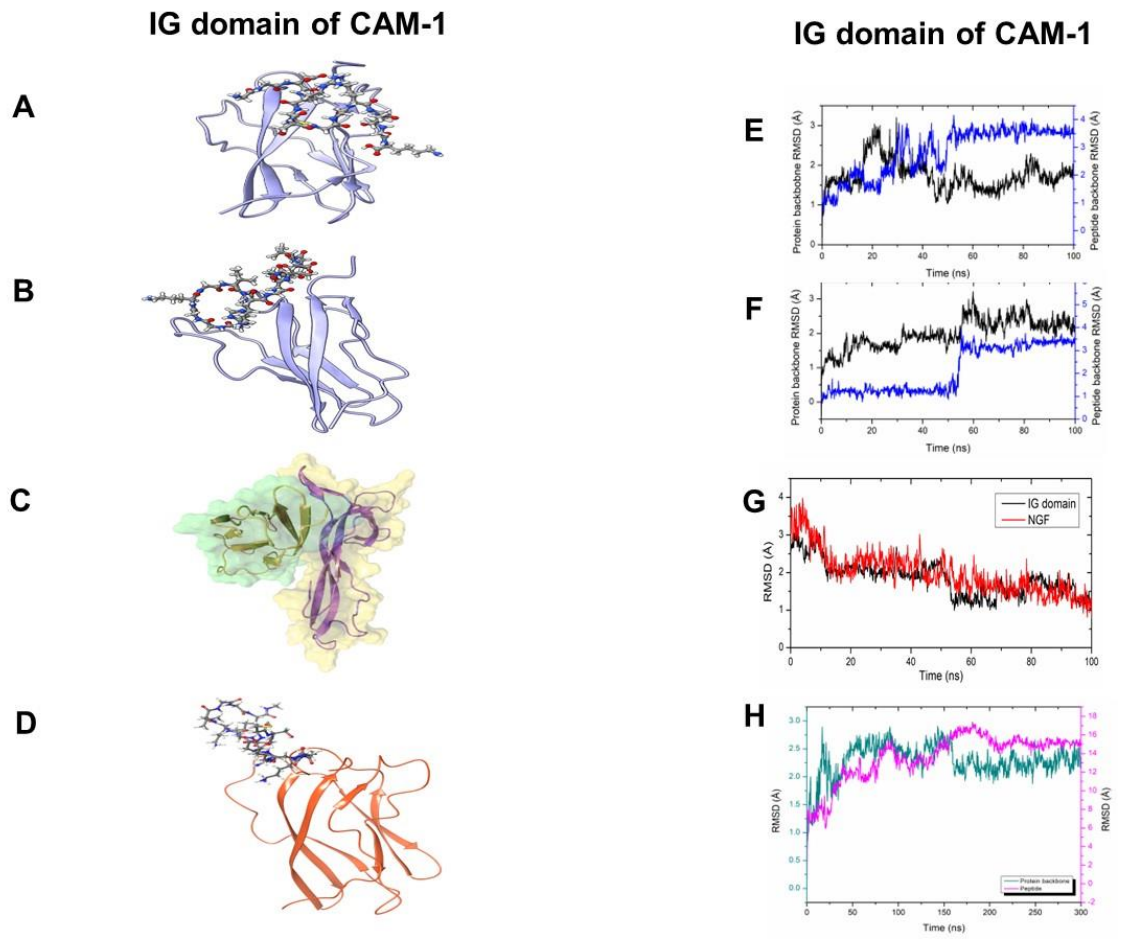

Fig. 5.1 Custom peptide (A) TNP, (B) HNP, (C) mouse-NGF, and (D) scrambled peptide complex with CAM1-IG domain shown in cartoon representation. Root mean square deviation (RMSD) plot of (E) TNP, (F) HNP, and (G) mouse-NGF, and (H) scrambled peptide complex complex with IG domain.

5.1.2 The confocal microscopic study shows *in vivo* binding of FITC–conjugated custom peptides to the nerve ring region of *C. elegans* N2 strain; however, an insignificant binding was observed with CAM-1 mutant strain of *C. elegans*

The confocal microscopic images of the dose-dependent (12.5 µg/mL to 100 µg/mL) and time-dependent (1h - 6 h) binding of the fluorescein isothiocyanate (FITC)-custom peptides (TNP and HNP) to *C. elegans* (L4 of N2 strain) are shown in Figs 5.2A-B and Figs 5.2C-D respectively. The FITC-custom peptides [50 µg/mL; 41.6 µM (TNP) and 35.7 µM (HNP)] showed binding at 2 h of incubation at the nerve ring part and hypodermal syncytia covering the lips and head portion of the *C. elegans* (Figs 5.2C-D). However, the FITC-bound scrambled peptide (50 µg/mL, 38.5 µM) did not shown

binding (2 h incubation) to the cam1 receptor at the nerve ring region of N2 worms (Figs 5.2E-F).

Pre-treatment of *C. elegans* with FITC-conjugated TNP and HNP showed optimum fluorescence intensity at the nerve ring region; nevertheless, only FITC-treatment (control) did not show fluorescence signal at the nerve ring region of *C. elegans*, indicating binding of peptides to the nerve ring region of *C. elegans* (Figs 5.2G-H). However, the post-addition of peptides after PT treatment showed a significant decrease in fluorescence intensity at the nerve ring region compared to custom peptides pre-treated worms before adding PT (Figs 5.2G-H). Further, when a fixed concentration of peptides was co-treated with increasing concentrations of PT, a PT concentration-dependent reduction in the fluorescence intensity at nerve ring regions was observed, suggesting custom peptides and mouse 2.5s NGF protect the nerve ring region of the *C. elegans* from PT-induced neuronal damage (Figs 5.2G-H).

Further, the binding efficiency of FITC-custom peptides (TNP and HNP) at their optimum dose (50 µg/mL) and time (2 h) in the N2 strain and CAM-1 mutant strain of *C. elegans* were compared in (Figs 5.3A-B). However, negligible binding was observed at the nerve ring region in the CAM-1 mutant strain of *C. elegans*, compared to the binding of FITC-custom peptides in the N2 strain of *C. elegans* which is evident by a significant ($p \leq 0.05$) decrease in the fluorescence intensity (19-27 %) of FITC-custom peptides was observed in the CAM-1 mutant strain when compared to the N2 strain of *C. elegans* (Fig 5.3B).

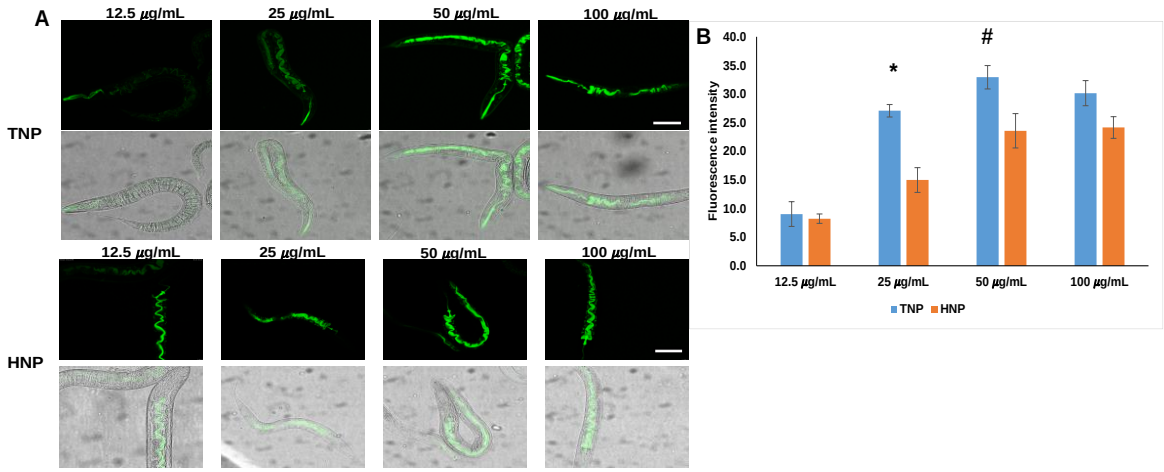

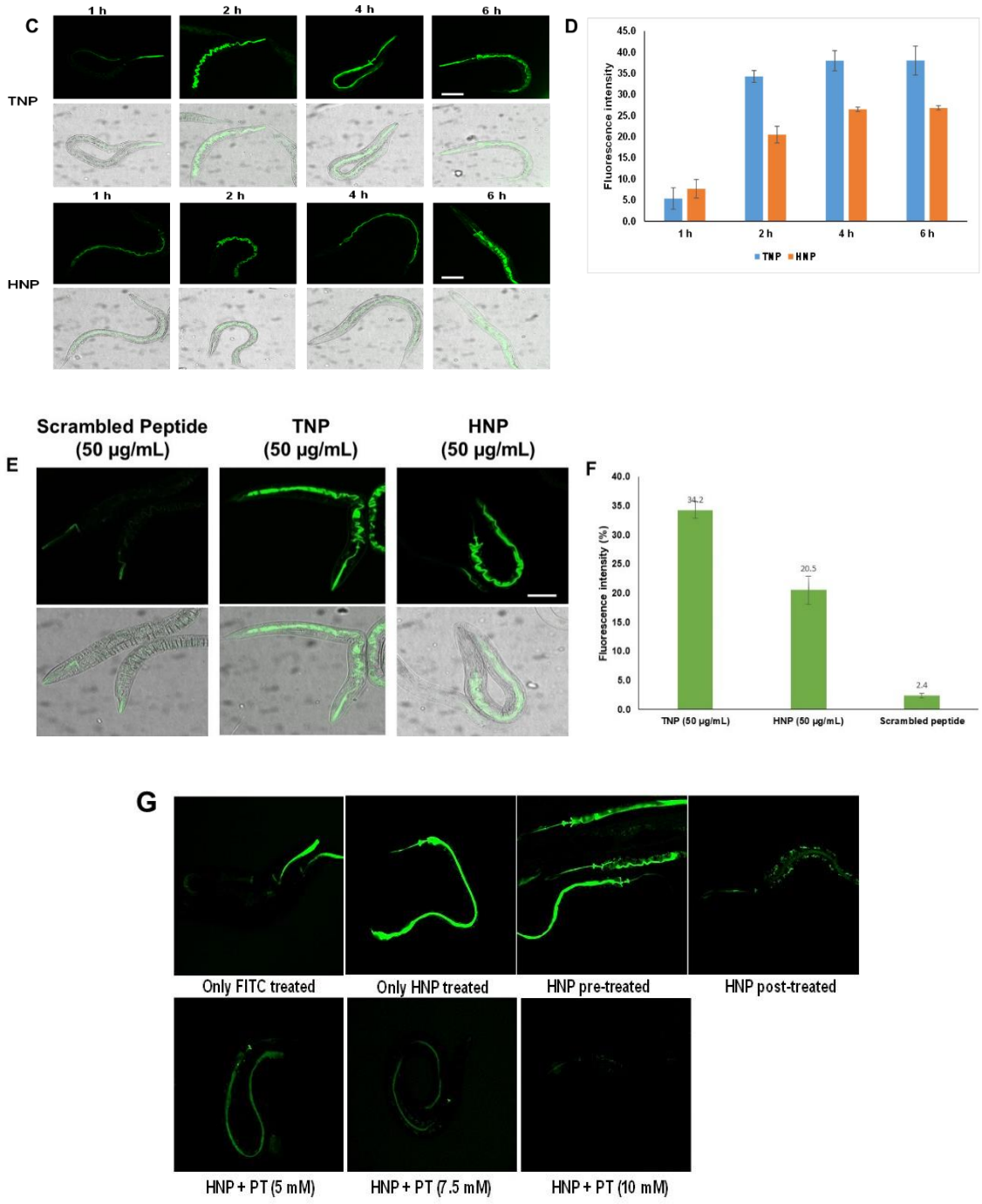
C
1 h
2 h
4 h
6 h
TNP
HNP
D
Fluorescence intensity
TNP
HNP
E
Scrambled Peptide (50 µg/mL)
TNP (50 µg/mL)
HNP (50 µg/mL)
F
Fluorescence intensity (%)
34.2
20.5
2.4
TNP (50 µg/mL)
HNP (50 µg/mL)
Scrambled peptide
G
Only FITC treated
Only HNP treated
HNP pre-treated
HNP post-treated
HNP + PT (5 mM)
HNP + PT (7.5 mM)
HNP + PT (10 mM)

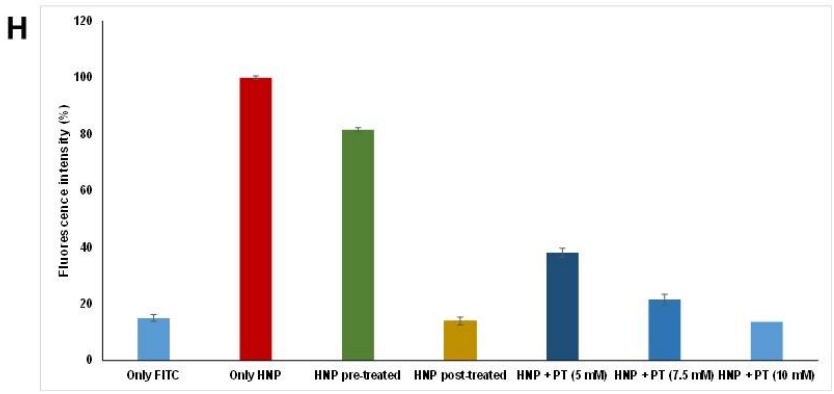

Fig. 5.2 Confocal microscopic (40 X) studies of the *in vivo* binding of FITC-custom peptides to *C. elegans* for 2h. (A) Dose-dependent (12.5 µg/mL to 100 µg/mL) binding of custom peptides to the *C. elegans*. The scale bar indicates the length as 100 µm. (B) Bar graph representing fluorescence intensity between the treatment groups; $^{*}p < 0.05$, a significant difference between 12.5 µg/mL and 25 µg/mL dose of FITC-conjugated peptides to *C. elegans*, $^{\#}p < 0.05$, a substantial difference between 25 µg/mL and 50 µg/mL dose of FITC-conjugated peptides to *C. elegans*. (C) Time-dependent (1 h – 4 h) binding of custom peptides (50 µg/mL) to the *C. elegans*. (D) Bar graph representing fluorescence intensity between the treatment groups (E) *In-vivo* binding of FITC-custom peptides and scrambled peptide to N2 *C. elegans*. (F) Bar graph illustrating fluorescence intensity between the FITC-custom peptides and FITC-scrambled peptide. The scale bar indicates the length as 100 µm. (G) Microscopic image of the custom peptide binding to *C. elegans* in pre-treatment, post-treatment, and co-treatment conditions (with various concentrations of PT). The scale bar indicates the length as 100 µm. (H) Bar graph representing fluorescence intensity between the treatment groups; Significant difference between the pre-treatment, post-treatment, and co-treatment with FITC-custom peptide HNP compared to binding of only FITC-conjugated HNP to *C. elegans*, $^{\#}p < 0.05$.

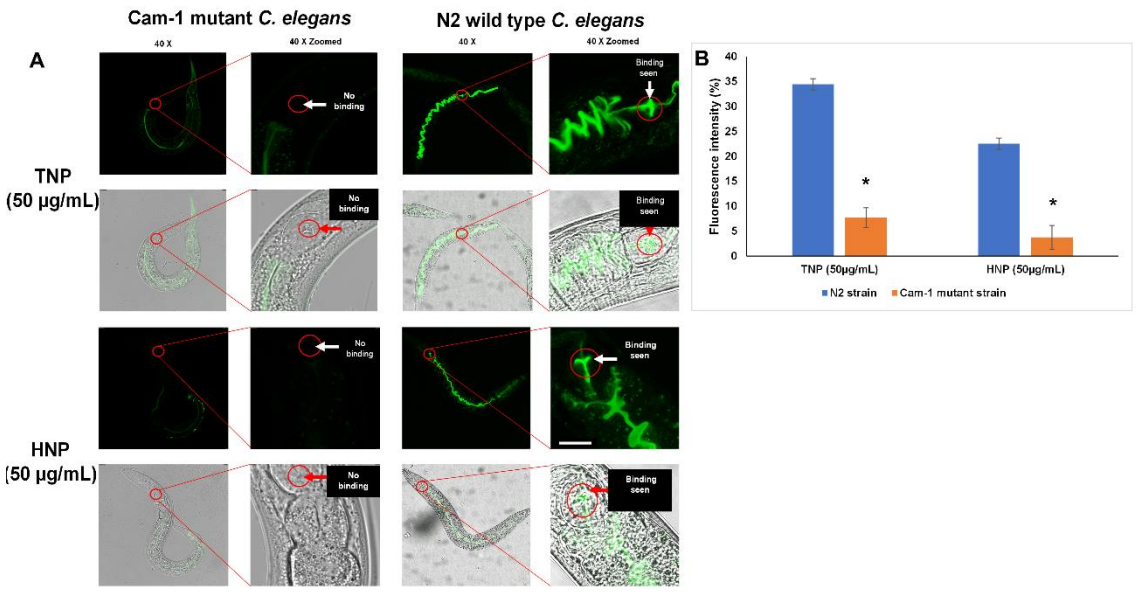

Fig. 5.3 (A) Confocal microscopic (40 X) studies of the *in vivo* binding of FITC-custom peptides (50 µg/mL, 2 h) to CAM-1 mutant and compared with wild-type N2 strain *C. elegans*. The scale bar indicates the length as 100 µm. (B) Bar graph representing fluorescence intensity between the CAM-1 mutant and N2 strains. $^{*}p < 0.05$, a significant difference between CAM-1 mutant and N2 strain of *C. elegans*. Values are mean ± SD of triplicate determinations.

5.1.3 Pre-treatment with custom peptides reduced PT-induced worms' death and restored their chemotaxis dysfunction

Custom peptides pre-treatment demonstrated a concentration-dependent increase (up to 50 µg/mL) in the survivability of the N2 strain of *C. elegans* against PT (LC_{50} value)-induced death, and the optimum concentration was determined for both the peptides at 50 µg/mL [41.6 µM (TNP) and 35.7 µM (HNP)] (Fig 5.4A). HNP showed a significant ($p \leq 0.05$) increase in survivability compared to TNP. Nevertheless, a wealth of data suggests that enhanced biological activity might not always follow from effective binding with the receptor [2,3]. The two peptides may exhibit varied inhibition against PT-induced toxicity due to their differing binding affinities and efficacies. The non-specific or unstable binding of peptides to the receptor may cause the binding efficiency and affinity variation. The antioxidant vitamin C (positive control; 100 µg/mL) pre-treated group showed minimal protective effect from death (Fig 5.4A).

Custom peptide pre-treatment for two hours showed a significant ($p \leq 0.05$) increase (35-40%) in the survivability of the N2 strain of untreated (control) *C. elegans* compared to PT-treated *C. elegans*; however, 12 h pre-treatment compared to 2 h pre-treatment was found to be less effective in protecting the *C. elegans* against PT-induced toxicity and death. Nevertheless, 12 h pre-treatment with custom peptides followed by re-supplementation of custom peptides again for 12 h (total pre-incubation time 24 h) restored the survivability of *C. elegans* against PT, and this result was found to be similar as shown by pre-incubation with custom peptides for 2 h before addition of PT (Fig 5.4B). Pre-treatment with 50 µg/mL quercetin, a known neuroprotection compound, demonstrated much lower protection than custom peptides under similar experimental conditions (Fig 5.4B).

However, post-treatment with custom peptides, vitamin C (antioxidant), mouse 2.5 S NGF, and quercetin (after PT addition) did not reverse the PT-induced toxicity in *C. elegans* (Fig 5.4C). Also, a significant ($p \leq 0.05$) decrease in the neutralization (23-27%) against paraquat-induced toxicity by custom peptides and mous-NGF pre-treatment in CAM-1 mutant strain was observed when compared to the N2 strain of *C. elegans* (Fig 5.4D). The pre-treatment with scrambled peptide did not show an increase in survivability compared to custom peptides (HNP and TNP) pre-treatment against PT-induced toxicity in *C. elegans* (Fig 5.4E).

No significant difference ($p \geq 0.05$) in the chemotaxis index (CI) between the peptide-treated and untreated (control) *C. elegans* was observed (Fig 5.4F). However, sensory neuron dysfunction was observed in PT-treated wild-type *C. elegans* (Fig 5.4F). Notably, a significant restoration ($p \leq 0.05$) of PT-induced sensory dysfunction was observed in pre- (CI = 0.43 ± 0.028 for TNP, and CI = 0.48 ± 0.024 for HNP) and post-peptide-treated worms (CI = 0.20 ± 0.014 for TNP, and CI = 0.24 ± 0.012 for TNP) compared to the worms treated with PT (Fig 5.4F). Further, pre- or post-treatment with vitamin C (antioxidant) is ineffective in improving PT-induced sensory neuron dysfunction (Fig 5.4F). Peptides TNP and HNP demonstrated similar potency ($p \geq 0.5$) in the restoration of PT-induced sensory neuron dysfunction in *C. elegans* (Fig 5.4F).

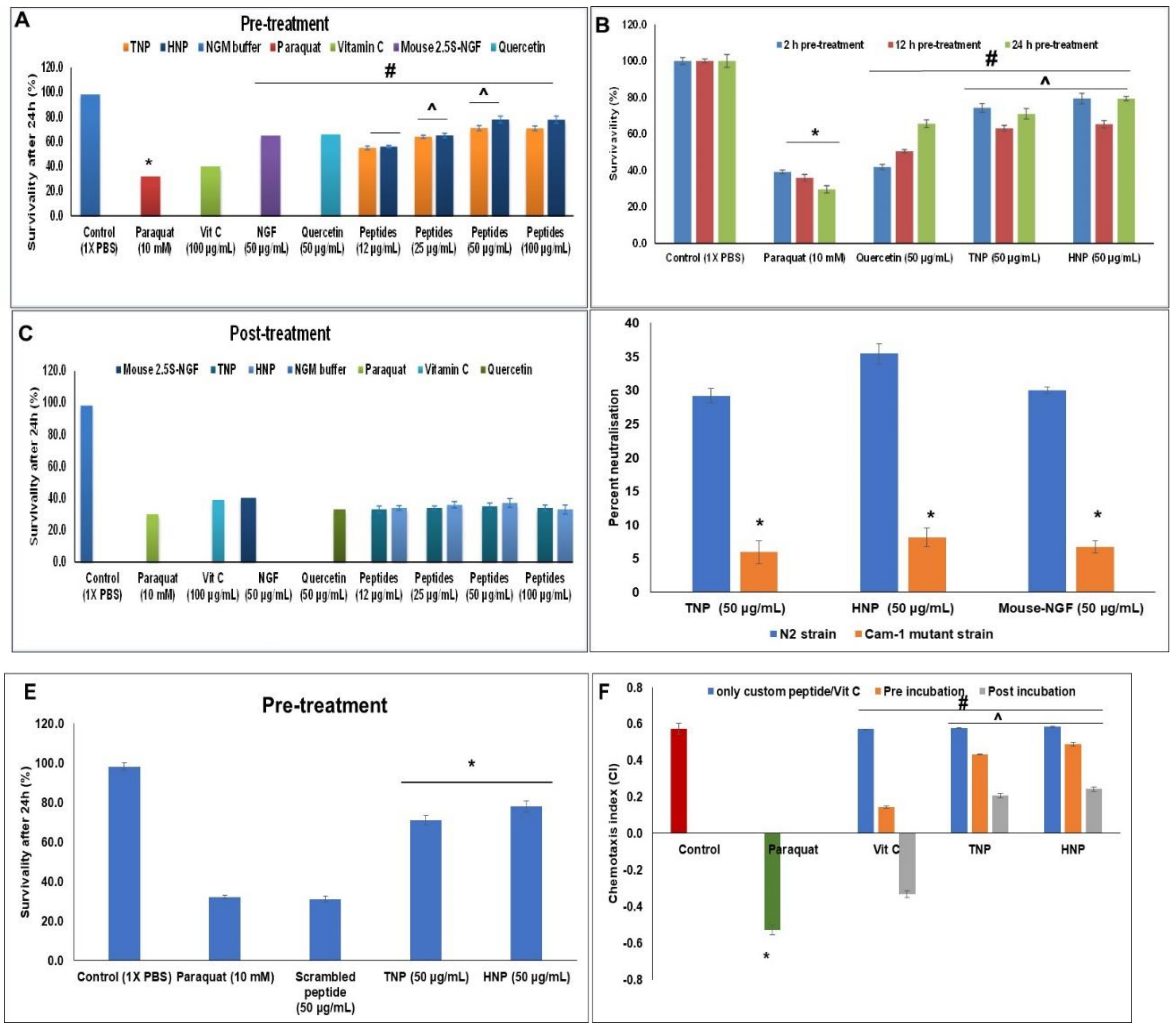

Fig. 5.4 Determination of the effect of the custom peptide on PT-induced death of *C. elegans*. (A) worms were pre-incubated with mouse 2.5S-NGF (50 µg/mL)/quercetin (50 µg/mL, positive control) / vitamin C (100 µg/mL, positive control) and progressive concentration of custom peptides (12 µg/mL - 100 µg/mL) followed by the PT (10 mM) treatment. $^{*}p \leq 0.05$, a significant difference between untreated (control) and PT-treated cells; $^{\#}p \leq 0.05$, a significant difference between PT-treated cells and quercetin/ mouse 2.5S-NGF/ vitamin C and custom peptide pre-treated *C. elegans*. $^{\wedge}p \leq 0.05$ Significance of difference in different concentrations for custom peptides. (B) worms were pre-incubated with quercetin (50 µg/mL, positive control) and custom peptides (50 µg/mL) for 2 h, 12 h, and 24 h followed by the PT (10 mM) treatment. $^{*}p \leq 0.05$, a significant difference between untreated (control) and PT-treated cells; $^{\#}p \leq 0.05$, a significant difference between PT-treated cells and quercetin (positive control) and custom peptide pre-treated *C. elegans*. $^{\wedge}p \leq 0.05$, a significant difference between quercetin pre-treated

C. elegans and the peptide (TNP and HNP) pre-treated *C. elegans*. (C) Worms were incubated with PT (10 mM) for 1 h and treated with custom peptides (12 µg/mL to 100 µg/mL). Freshly prepared custom peptides were added after 12 h of pre-incubation for 24 h pre-incubation condition. Worms were counted under a stereo zoom microscope for 30 s up to 24 h of treatments. Values are mean ± SD of triplicate determinations. (D) Determination of the effect of the custom peptides on PT-induced death of cam-1 mutant compared with wild type N2 strain of *C. elegans*. Worms were pre-incubated with custom peptides (50 µg/mL) followed by the PT (10 mM) treatment. Percent neutralization was calculated against only paraquat-treated worms. $^{*}p < 0.05$, a significant difference between wild-type and cam-1 mutant strain. (E) Determination of the effect of the custom peptides and scrambled peptide on PT-induced death of wild type N2 strain of *C. elegans*. worms were pre-incubated with custom peptides/scrambled peptide (50 µg/mL) followed by the PT (10 mM) treatment. Percent survivability was calculated against only paraquat-treated worms. $^{*}p < 0.05$, a significant difference between only paraquat treated group and custom peptide (TNP, HNP). (F) Restoration of chemosensory behavior in *C. elegans* pre-treated with custom peptides. Synchronized L4 stage *C. elegans* wide-type strain N2 was incubated with or without 50 µg/mL custom peptides. They were then subjected to PT-treatment (10 mM) and a chemosensory assay. $^{*}p \leq 0.05$, a significant difference between untreated (control) and PT-treated cells; $^{\#}p \leq 0.05$, a significant difference between PT-treated cells and quercetin (positive control) and custom peptide pre-treated *C. elegans*. $^{\wedge}p \leq 0.05$, a significant difference between quercetin pre-treated *C. elegans* and the peptide (TNP and HNP) pre-treated *C. elegans*. Values are means ± SD of triplicate determinations.

5.1.4 Custom peptides inhibit PT-induced reactive oxygen species (ROS) production and depolarization of mitochondrial membrane potential in *C. elegans* N2 strain but could not protect CAM-1 mutant strain

The spectrofluorometric determination of fluorescence intensity of DCF (2,7-dichlorofluorescein) confirmed a significant ($p \leq 0.05$) increase in the ROS level in PT (10 mM)-treated wild-type worms by 44% compared to control (untreated) worms. A significant reduction ($p \leq 0.05$) in ROS level was observed in wild-type worms pre-treated with HNP and TNP (68-70%) and vitamin C (35%), mouse 2.5S-NGF (33%) as compared

to the PT-treated wild type worms (Fig 5.5A). The custom peptide HNP at a concentration of 50 µg/mL [41.6 µM (TNP) and 35.7 µM (HNP)] showed superior reduction (32-35%) ($p \leq 0.05$) in the ROS generation, compared to TNP and vitamin C (positive control) (Fig 5.5A).

The confocal microscopic analysis also determined the custom-peptides mediated reduction in intracellular ROS generation in wild-type N2 strain *C. elegans* (Figs 5.5B-C). The data showed a significant increase ($p \leq 0.05$) in intracellular ROS levels in PT-treated worms compared to control wild-type worms. Further, pre-treatment of worms with custom peptides (TNP and HNP, 50 µg/mL) and vitamin C (positive control, 100 µg/mL) /mouse 2.5S-NGF (50 µg/mL) significantly diminished the ROS production (Fig 5.5C); however, to a different extent. Custom peptide HNP, compared to TNP, showed superior activity in inhibiting PT-induced ROS production in wild-type worms (Fig 5.5C). No significant ($p \geq 0.05$) decrease in ROS production was observed in the custom peptides pre-treatment group compared to the PT-treated group in the CAM-1 mutant strain of *C. elegans* (Figs 5.5D-E).

The JC-1 staining procedure was used to study whether custom peptides can restore the loss of mitochondrial membrane potential (MMP) triggered by PT in *C. elegans* N2 and CAM-1 mutant strains. The effect of custom peptides on MMP using JC-1 dye (cyanin dye) (Fig 5.5D) was demonstrated. The red/green fluorescence ratio was quantified from the confocal images to monitor the MMP (Fig 5.5F). The fluorescence intensity of the red/green ratio was significantly reduced ($p \leq 0.05$) by 80% in 10 mM PT-treated worms compared to control (1X PBS-treated) worms (Fig 5.5F). However, the fluorescence intensity of the red/green ratio was significantly ($p \leq 0.05$) restored by 60 to 70% when worms were pre-treated with custom peptide (TNP / HNP) as compared to PT-treated worms (Figs 5.5F-G), indicating a reduction of PT-induced depolarization of MMP by custom peptides in *C. elegans*. HNP showed a significant ($p \leq 0.05$) 20% increase in the restoration of PT-induced mitochondrial depolarization as compared to TNP (Figs 5.5F-G). In contrast, vitamin C pre-treatment showed no significant difference in the restoration of PT-induced mitochondrial depolarisation (Figs 5.5F-G). Moreover, custom peptide pre-treatment did not offer any considerable repair of alteration of MMP in the CAM-1 mutant strain of *C. elegans* (Figs 5.5H-I).

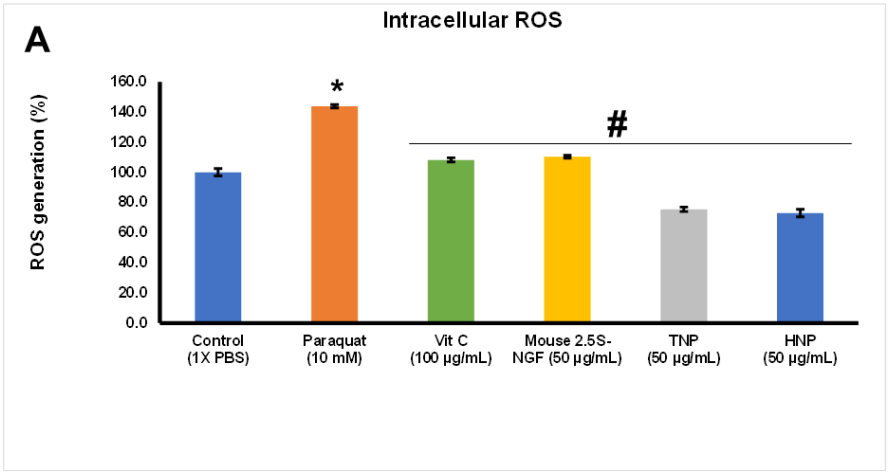
A
Intracellular ROS
ROS generation (%)
160.0
140.0
120.0
100.0
80.0
60.0
40.0
20.0
0.0
*
#
Control (1X PBS)
Paraquat (10 mM)
Vit C (100 µg/mL)
Mouse 2.5S-NGF (50 µg/mL)
TNP (50 µg/mL)
HNP (50 µg/mL)

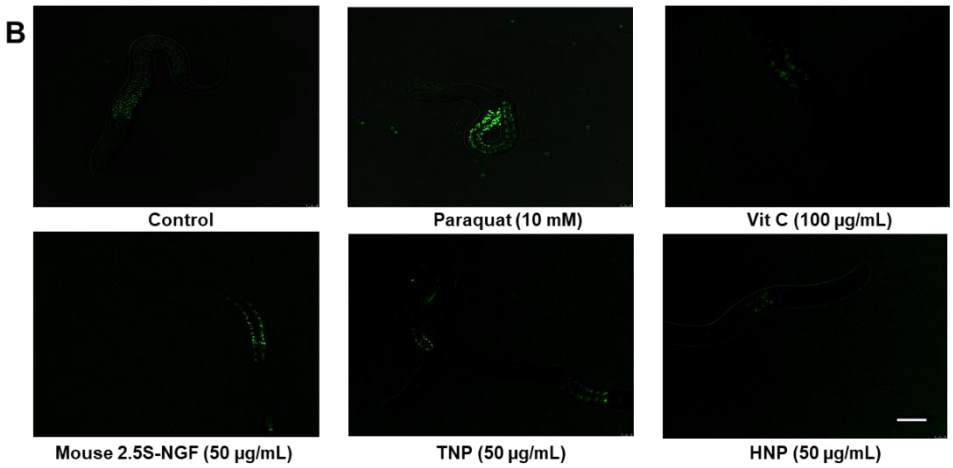
B
Control
Paraquat (10 mM)
Vit C (100 µg/mL)
Mouse 2.5S-NGF (50 µg/mL)
TNP (50 µg/mL)
HNP (50 µg/mL)

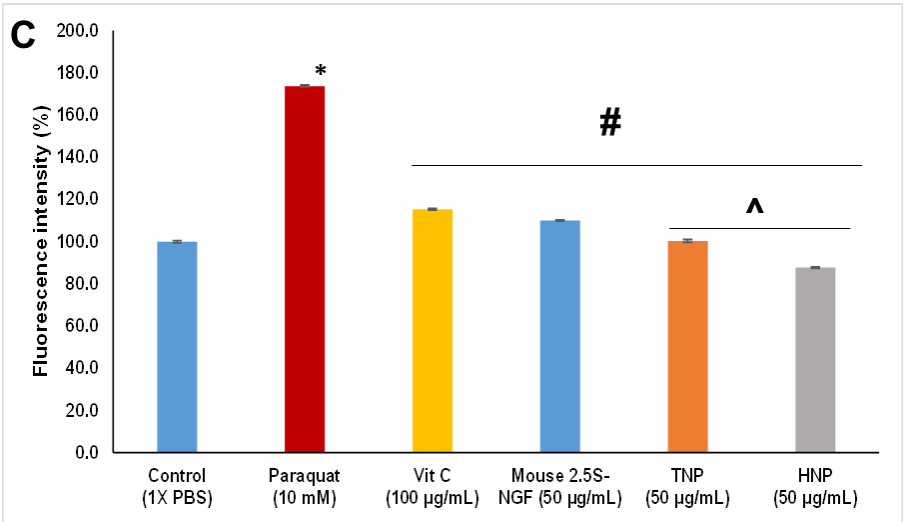
C
Fluorescence intensity (%)
200.0
180.0
160.0
140.0
120.0
100.0
80.0
60.0
40.0
20.0
0.0
*
#
^
Control (1X PBS)
Paraquat (10 mM)
Vit C (100 µg/mL)
Mouse 2.5S-NGF (50 µg/mL)
TNP (50 µg/mL)
HNP (50 µg/mL)

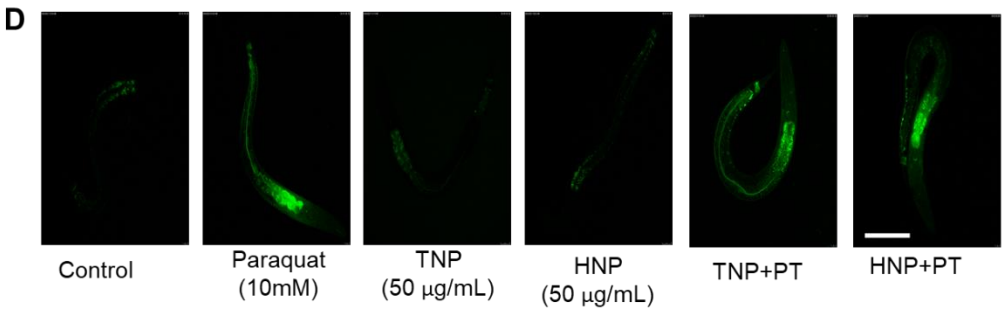
D
Control
Paraquat (10mM)
TNP (50 µg/mL)
HNP (50 µg/mL)
TNP+PT
HNP+PT

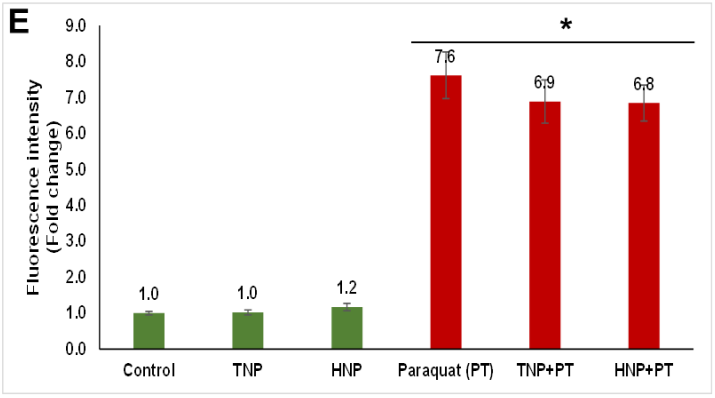
E
Fluorescence intensity (Fold change)
9.0
8.0
7.0
6.0
5.0
4.0
3.0
2.0
1.0
0.0
*
7.6
6.9
6.8
1.0
1.0
1.2
Control
TNP
HNP
Paraquat (PT)
TNP+PT
HNP+PT

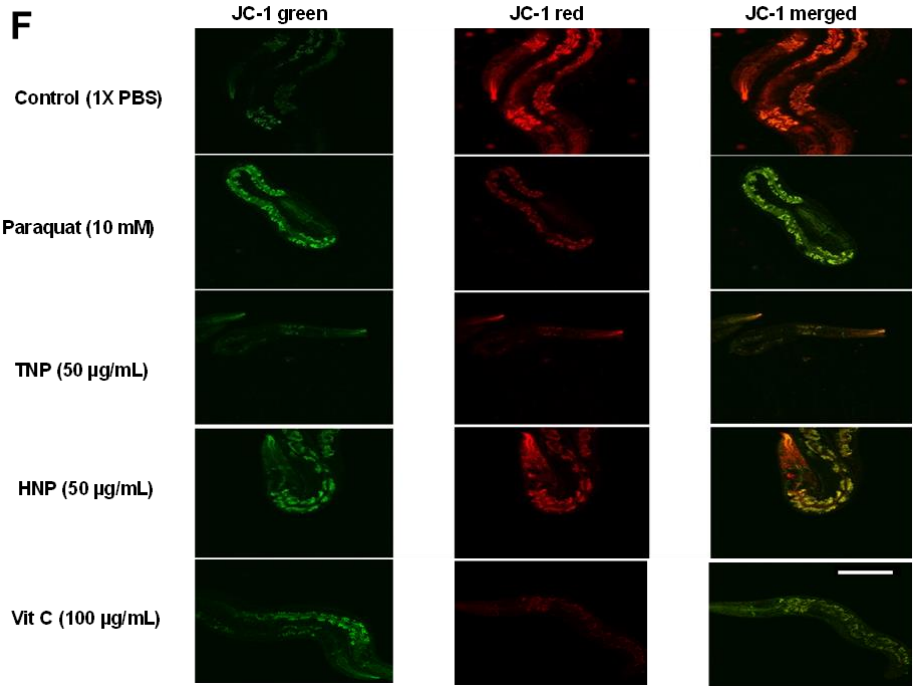
F
JC-1 green
JC-1 red
JC-1 merged
Control (1X PBS)
Paraquat (10 mM)
TNP (50 µg/mL)
HNP (50 µg/mL)
Vit C (100 µg/mL)

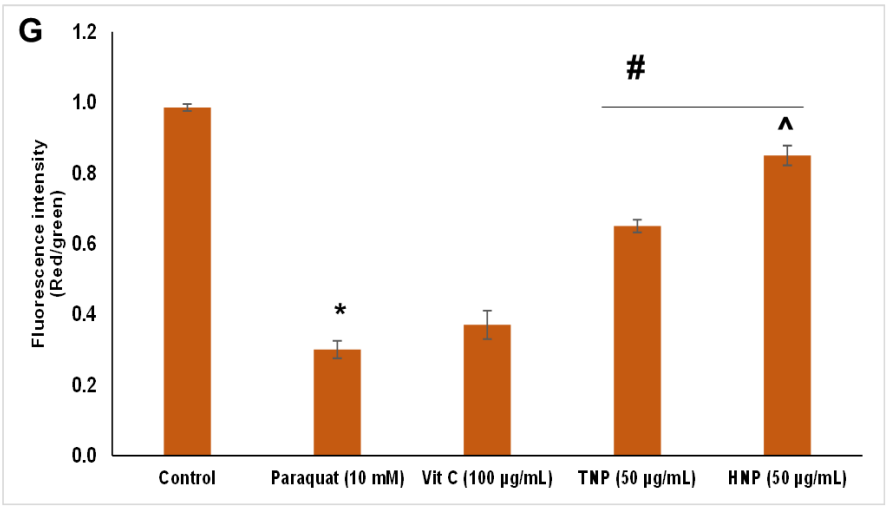

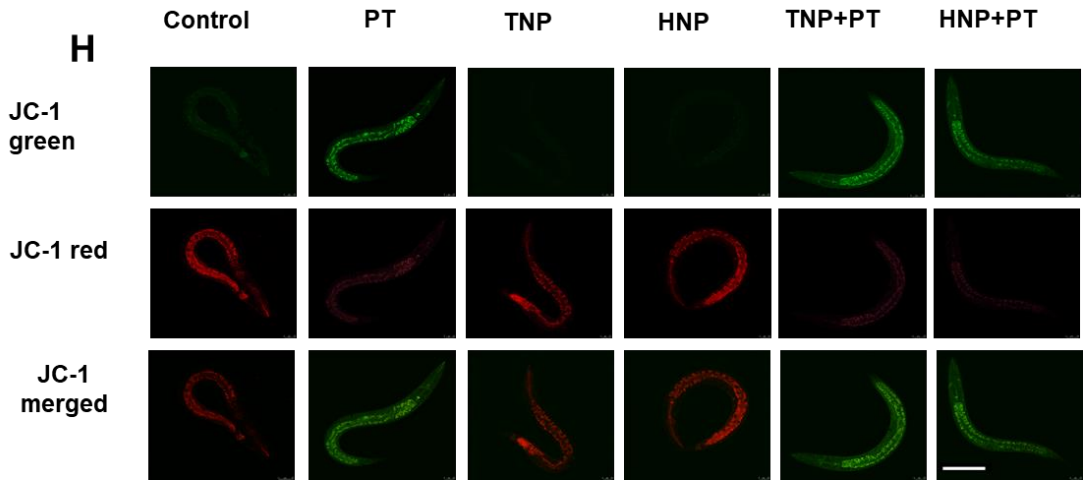

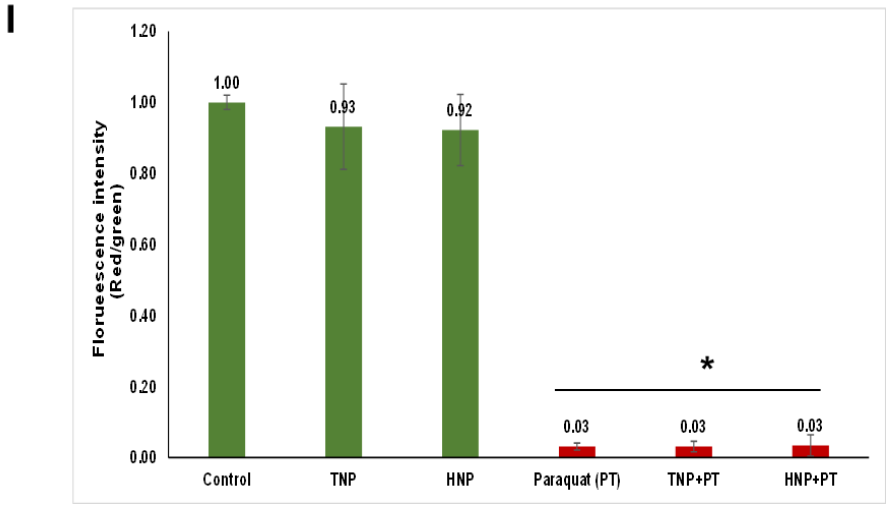

Fig. 5.5 Determination of PT-induced intracellular ROS generation and its reversal by pre-treatment with custom peptide in wild type N2 strains of *C. elegans.* The ROS generation was determined by using an H_2DCFDA fluorescence probe. (A)

spectrofluorometric determination of intracellular ROS. $^{*}p < 0.05$, the significant difference between untreated (control) and PT-treated worms; $^{\#}p < 0.05$, the significant difference between PT-treated and custom peptide-treated worms. (B) confocal microscope images of nematodes expressing ROS. The scale bar indicates the length as 100 µm. (C) Bar graph representing dosimetry analysis of confocal images to quantitate the intracellular ROS generation. Error bars indicating SD (n=3). $^{*}p < 0.05$, the significant difference between untreated (control) and PT-treated worms; $^{\#}p < 0.05$, the significant difference between PT-treated and custom peptide-treated worms. $^{\wedge}p \leq 0.05$, a significant difference between Vit C/ mouse 2.5 S-NGF pre-treated *C. elegans* and the peptides (TNP and HNP) pre-treated *C. elegans*. Values are means ± SD of triplicate determinations. (D) confocal microscope images of nematodes expressing ROS. The scale bar indicates the length as 100 µm. (E) Bar graph representing dosimetry analysis of confocal images to quantify intracellular ROS generation.

(F) Confocal images of *C. elegans* showing reversal of PT-induced disruption of mitochondrial membrane potential (MMP) of *C. elegans* pre-treated with custom peptides. The scale bar indicates the length as 100 µm. The scale bar indicates the size as 100 µm. The PT-treated (10 mM) N2 wild-type strain of nematodes pre-treated with or without custom peptide (50 µg/mL) was observed to measure the red/green fluorescence intensity ratio by JC-1 staining. (G) Bar diagram representing the red/green fluorescence intensity ratio quantified using Image J software. $^{*}p \leq 0.05$, a significant difference between untreated (control) and PT-treated worms; $^{\#}p \leq 0.05$, a significant difference between PT-treated and custom peptide pre-treated worms. $^{\wedge}p \leq 0.05$, a significant difference between the two peptides (TNP and HNP) pre-treated *C. elegans*. Values are means ± SD of triplicate determinations. (H) Confocal images of CAM-1 mutant strain of *C. elegans* showing reversal of PT-induced disruption of mitochondrial membrane potential (MMP) of *C. elegans* pre-treated with custom peptides. The scale bar indicates the length as 100 µm. The scale bar indicates the size as 100 µm. The PT-treated (10 mM) N2 wild-type strain of nematodes pre-treated with or without custom peptide (50 µg/mL) was observed to measure the red/green fluorescence intensity ratio by JC-1 staining. (I) Bar diagram representing the red/green fluorescence intensity ratio quantified using Image J software. $^{*}p \leq 0.05$, a significant difference between untreated (control)/only

custom peptide treated group and PT/custom peptide and PT-treated group of cam-1 mutant worms

5.1.5 Custom peptides restored PT-induced dopaminergic (DAergic) neurodegeneration and reduced *α*-synuclein accumulation in *C. elegans*

C. elegans BZ555 strain expresses a green fluorescent protein in all six intact DAergic neurons comprising two distal cephalic (CEPD), two ventral cephalic (CEPV), and two anterior deirid (ADE) (Fig 5.6A). Studies have shown that specific DAergic neuron degeneration is attained with 10 mM PT exposure [4-6], which showed impairment of CEPs and ADEs cell bodies (Fig 5.6B). The analysis showed a significant decrease ($p \leq 0.05$) in the fluorescence intensity with PT treatment by 54-58% for CEPs and 70-75% for ADEs neurons compared with the PBS-treated (control) worms (Fig 5.6B). The TNP and HNP peptides pre-treated groups showed a significant ($p \leq 0.05$) increase in fluorescence intensity for CEPs neurons and ADEs neurons (Figs 5.6A-B). This data suggests a considerable impairment of PT-induced neuronal degeneration and significantly higher activity of HNP as compared to TNP (Figs 5.6A-B). However, the vitamin C pre-treated group does not show a significant ($p > 0.05$) increase in fluorescence intensity for CEPs and ADEs neurons compared with the PT-treated worms (Figs 5.6A-B). Similarly, peptides TNP and HNP in post-treated worm groups showed a significant ($p \leq 0.05$) increase in GFP intensity by 57.5-59.3% and 60.3-63.7%, respectively, for CEPs neurons and 38.5% and 65%, for ADES neurons (Figs 5.6A-B). Fluorescence intensity statistics were used to analyze alterations in dopaminergic neurons after CP treatment. Furthermore, the evidence indicates that ADE neurons are somewhat more successfully restored by post-treatment than CEP neurons. Consequently, there is some effectiveness during pre-treatment and following it.

The fluorescence intensity at the anterior part of the NL5901 strain of *C. elegans* showed aggregation of human *α*-synuclein (YFP tagged) in the body wall muscles (Fig 5.6C). The image analysis showed a significant decrease ($p \leq 0.05$) in the fluorescence intensity in the custom peptides-treated *C. elegans* as compared with the PBS-treated (control) *C. elegans* (Fig 5.6D). The TNP and HNP treatment showed a significant ($p \leq 0.05$) decrease in the fluorescence intensity by 37% and 60%, respectively, compared to the fluorescence intensity of the control (untreated) group of worms (Figs 5.6C-D). HNP

treatment, compared to the TNP treatment, showed a significant ($p \leq 0.05$) 20% decrease in the *α*-synuclein accumulation in *C. elegans* (Figs 5.6C-D). However, vitamin C pre-treatment did not show a significant ($p > 0.05$) reduction in the *α*-synuclein accumulation, as compared to the PBS-treated (control) group of *C. elegans* (Figs 5.6C-D).

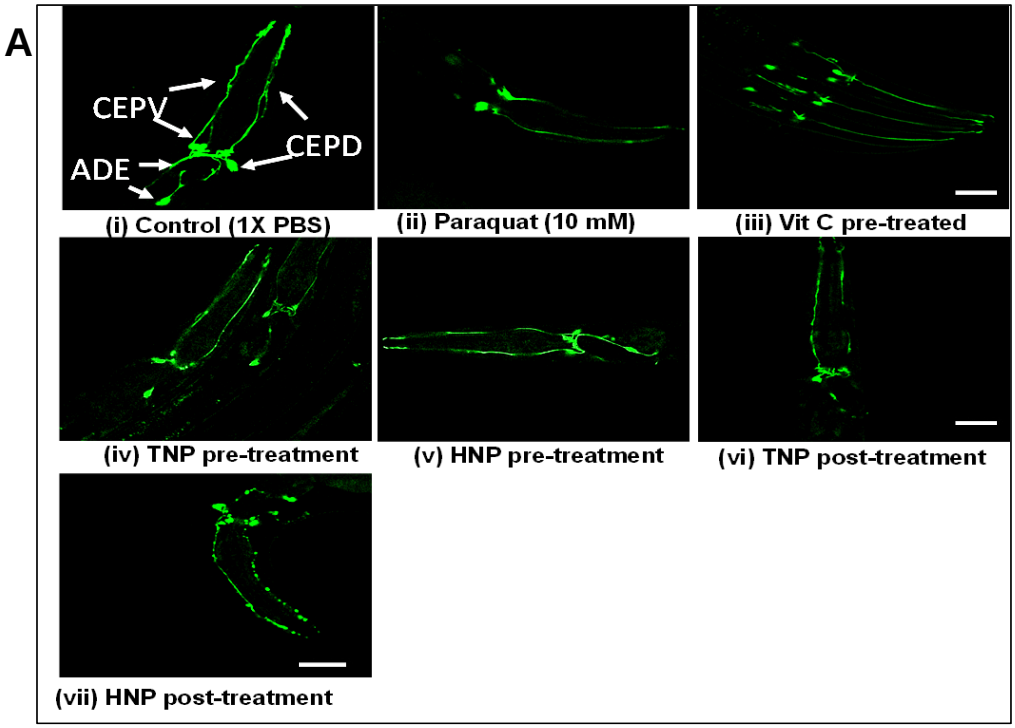

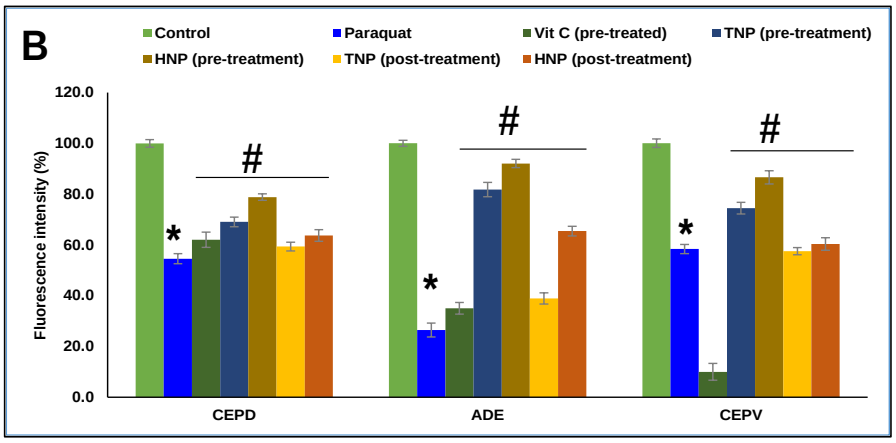

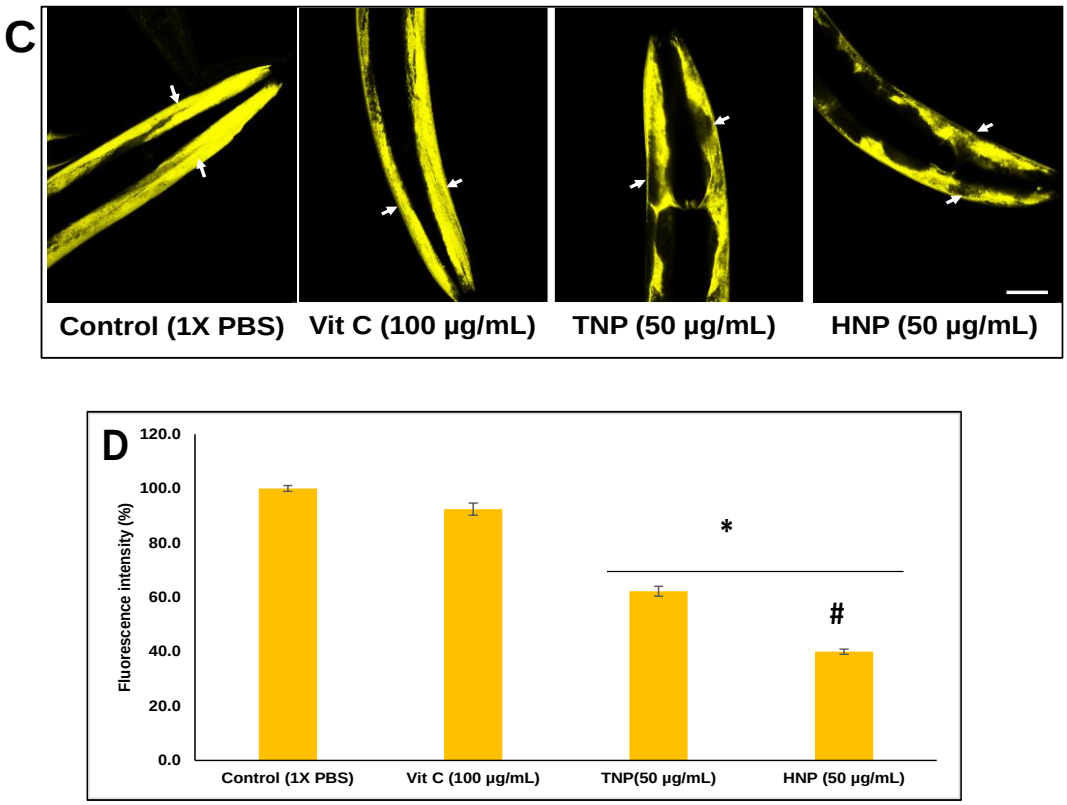

Fig. 5.6 determination of dopaminergic neurodegeneration induced by PT in BZ555 *C. elegans*. (A) Confocal microscopic images (40 X) of DA neurons emerging GFP fluorescence signals in PT-treated BZ555 worms with or without pre-treated with custom peptides (50 µg/mL). The scale bar indicates the length as 100 µm. (B) The bar diagram shows the GFP fluorescence intensity indicating the content of DA neurons in BZ555 worms, quantified using the Image J software. $^{*}p \leq 0.05$, a significant difference between untreated (control) and PT-treated worms; $^{\#}p \leq 0.05$, a significant difference between PT-treated and custom peptide-treated worms. Custom peptides inhibit the aggregation of *α*-synuclein in transgenic NL5901 strains of *C. elegans*. (C) Confocal images of custom peptides (50 µg/mL)-treated NL5901 worms after 12 h of incubation. The scale bar indicates the length as 100 µm. (D) The bar chart shows the fluorescence intensity representing the *α*-synuclein protein accumulation in custom peptide-treated NL5901 worms for 12 h. * ($p \leq 0.05$) a significant difference between control (CT) and custom peptides-treated *C. elegans*, $^{\#}$ ($p \leq 0.05$) a significant difference between TNP and HNP treated *C. elegans*. Values are means ± SD of triplicate determinations.

5.1.6 The custom peptides pre-treatment restores the PT-induced upregulated antioxidant/heat shock response/ p38 mitogen-activated protein kinase (MAPK) genes and delayed PT-induced programmed cell death in *C. elegans*

The quantitative reverse transcription-polymerase chain reaction (qRT-PCR) analysis data demonstrated a significant increase ($p \leq 0.05$) in the expression of antioxidant genes (*sod-1, sod-3, cat-1, cat-3, trx-1*, *gst-4*, and *gst-6)*, heat shock gene *hsp-16.1*, and MAPK signaling pathways genes (*skn-1*, *sek-1*, and *pmk-1)* in PT-treated N2 worms compared to untreated worms (control). However, pre-treatment of worms with vitamin C (positive control) / custom peptides (HNP and TNP) resulted in a significant restoration ($p \leq 0.05$) of the expression of those genes upregulated by PT treatment (Fig 5.7).

Although the binding sites of both custom peptides are the same, they have different molecular weights and lengths. Further, they were designed from two species of snake venom (Indian cobra and Russel's viper). Therefore, the efficacy and mechanism of action for both custom peptides can be different. This data is an exciting finding that both peptides ultimately showed antioxidant and neuroprotective potential, either by enhancing the fold change of antioxidant enzymes to eliminate free radicals in response to PT toxicity or improving the fold change of stress resistance against PT toxicity. (Fig 5.7).

Further, the qRT-PCR analysis also showed significant ($p \leq 0.05$) upregulation of pro-apoptotic genes (*ced-3* and *ced-4*) and significant downregulation ($p \leq 0.05$) of antiapoptotic genes (*ced-9*) in PT-treated *C. elegans* compared to untreated (control) *C. elegans*. Further, the pre-treatment of custom peptides (TNP and HNP) restores the upregulated (*ced-3* and *ced-4*) and downregulated (*ced-9*) pro-apoptotic and antiapoptotic genes, respectively, in PT-treated *C. elegans* (Fig 5.7). However, vitamin C (positive control) pre-treatment did not show significant down-regulation ($p \leq 0.05$) of MAPK signaling pathway genes (*skn-1*, *sek-1*, and *pmk-1)* and pro-apoptotic genes (*ced-3* and *ced-4*) compared to PT-treated worms (Fig 5.7). Further, the qRT-PCR analysis showed better activity of HNP compared with TNP. Therefore, HNP was selected for the transcriptomic and proteomics analyses to decipher the gene regulatory pathways for preventing PT-induced neuronal degradation.

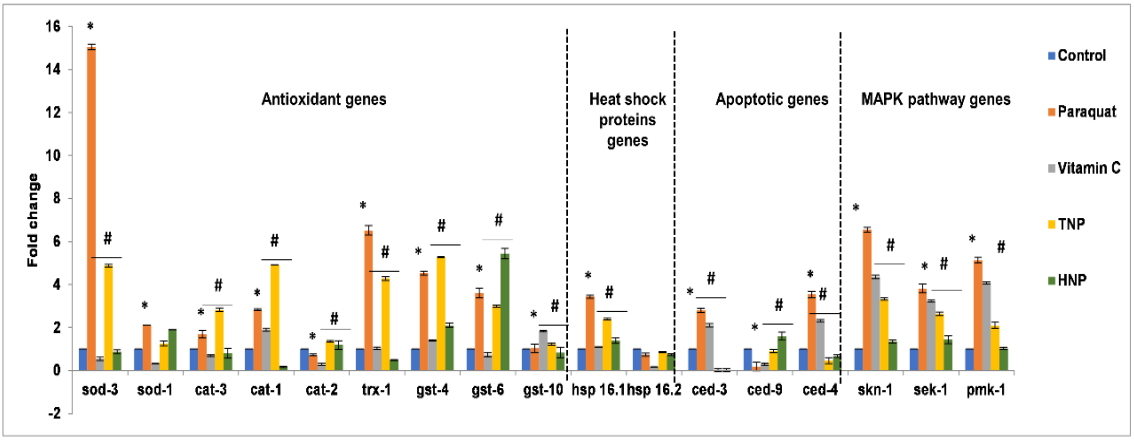

Fig. 5.7 The qRT-PCR analysis shows the genes' expression in stress resistance, innate immunity, and apoptotic pathways in the PT-treated *C. elegans*, compared with the vitamin C (positive control)/custom peptide pre-treated *C. elegans*. The expression of mRNA was normalized using the housekeeping gene act-1. * ($p \leq 0.05$) a significant difference between control (CT) and PT-treated *C. elegans*, $^{\#}$ ($p \leq 0.05$) a significant difference between PT-treated and vitamin C/ custom peptide pre-treated worms. Values are means ± SD of triplicate determinations.

5.1.7 Transcriptomic analysis shows the differential expression of mRNA between PT-treated *C. elegans* and pre-treatment of *C. elegans* with custom peptides followed by PT-treatment

The cDNA libraries were prepared for the mRNA, isolated from each group of *C. elegans* (N2*)* treated with (a) 1X PBS (control) treated worms (CT group), (b) 10 mM PT treatment for 1 h (PT group), (c) pre-treatment with 50 µg/mL [41.6 µM (TNP) and 35.7 µM (HNP)] custom peptide HNP for 2 h followed by 10 mM PT treatment for 1 h (PHNP group), and (d) treatment with 50 µg/mL of custom peptide HNP for 2 h (HNP group). The mRNAs were sequenced with the Illumina 150 bp PE platform. The average total number of reads aligned was found to be 16.7 million (CT), 15.3 million (HNP), 12.8 million (PHNP), and 20.2 million (PT) for the three corresponding cDNA libraries.

The transcriptomic analysis showed differential expression of 15,102 genes in *C. elegans* compared to the PT and CT group of worms and 701 genes when compared between the PT and PHNP group, in which 441 and 260 genes were found to be upregulated and downregulated, respectively.

The transcriptomic data's principal component analysis (PCA) revealed variance in the gene expression level between all four treatment groups (Fig 5.8A). The correlation plot (Fig 5.8B) shows clustering among different treated groups. Red indicates the positive, and blue indicates the negative correlation plot between the four treatment groups (Fig 5.8B). The volcano (p-values vs. fold change) and scatter plots display the (i) differential gene expression between PT and CT groups (Figs 5.8C-D) and (ii) differentially altered genes between PHNP and PT groups (Figs 5.8E-F). The Volcano plot and scatter plot analyses revealed significant downregulation (Fc < -1) of most of the genes in *C. elegans* in the PT group compared to the CT group. The pre-treatment of peptide (HNP) resulted in the upregulation of those 'genes' expression downregulated in the PT group of worms (Figs 5.8C-F). The heat map analysis displayed a disparity in gene expression between the PT and PHNP groups compared to the CT group (Fig 5.8G).

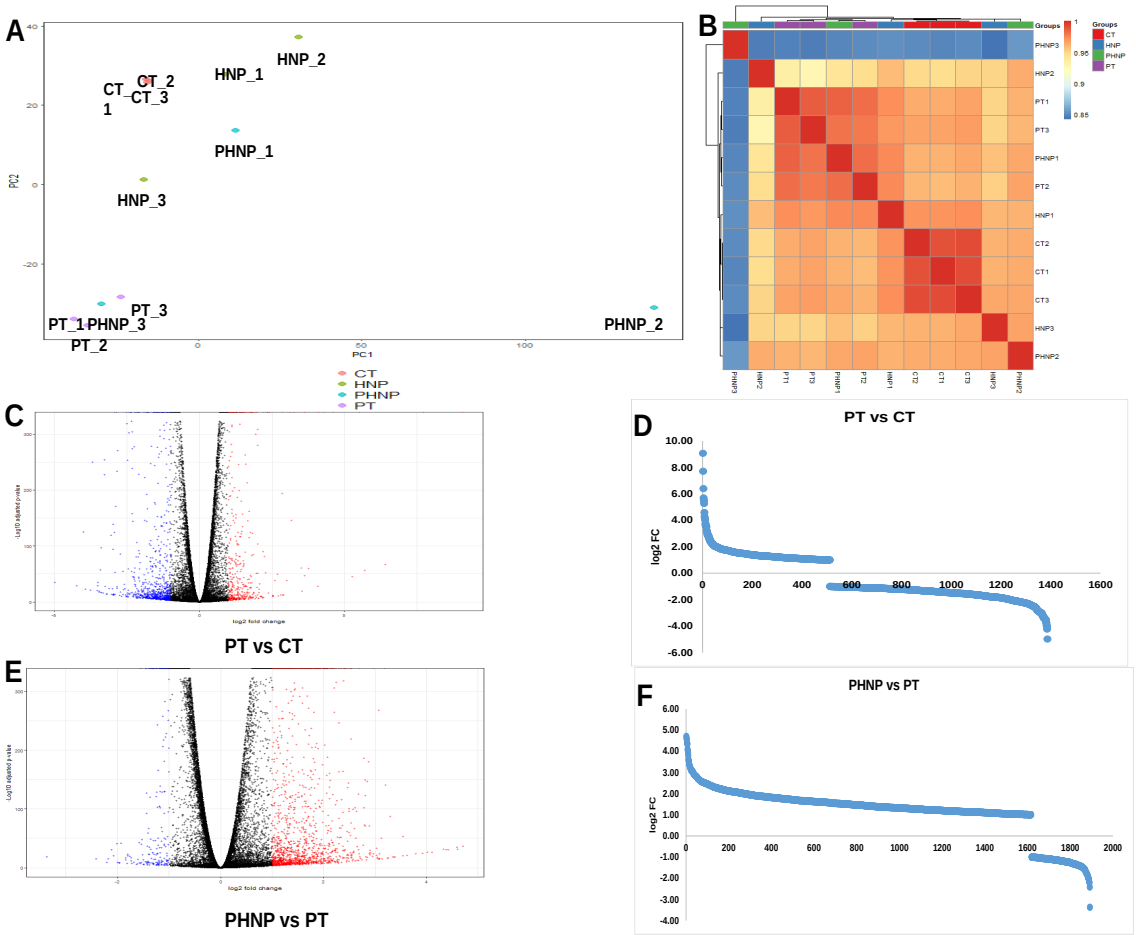

G

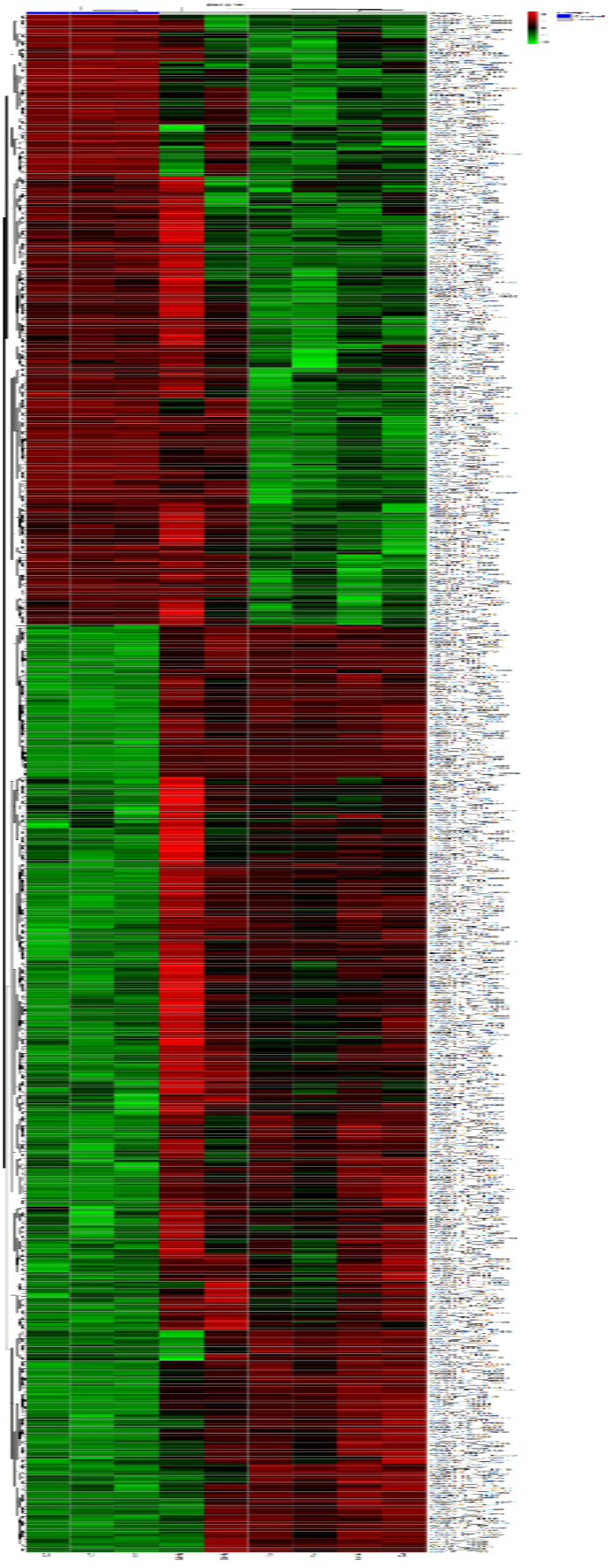

Fig. 5.8 Differential expression of genes between different treated groups of *C. elegans*. (A) PCA score plot showing the gene expression variability between the groups of *C. elegans* and within the biological replicates. (B) Correlation plot showing a correlation between treated groups of *C. elegans*. CT: untreated worms, PT: PT treated worms, PHNP: custom peptide HNP pre-treatment followed by PT treatment, HNP: custom peptide HNP treated worms. Plots showing differential expression of genes in PT-treated *C. elegans* and their restoration with peptide (HNP) pre-treatment. (C) Volcano plot (p-value v/s log Fc) for PT group versus CT group. (D) scatter plot displaying the statistically significant differentially altered genes between PT treatment and control group (PT vs. CT). (E) Volcano plot (p-value v/s log Fc) for PHNP group versus PT group (F) scatter plot displaying the statistically significant differentially altered genes between peptide HNP pre-treated *C. elegans* followed by PT treatment and PT-treated *C. elegans*. CT: untreated worms, PT: PT treated worms, PHNP: custom peptide HNP pre-treatment followed by PT treatment, HNP: custom peptide HNP treated worms. (G) Heat map showing the differential expression of the upregulated and downregulated genes among different groups of *C. elegans*. PT: PT treated, PHNP: peptide HNP pre-treatment followed by PT treatment, CT: untreated (control) worms.

5.1.8 Quantitative proteomic analysis demonstrated differential expression of cellular proteins between PT-treated and HNP peptide pre-treated followed by PT-treated *C. elegans*

A total number of 1026 non-redundant proteins were identified by the LC-MS/MS analysis from the different treatment groups of *C. elegans* (N2 strain). The identified proteins were classified into 20 discrete categories based on their cellular location and biological activity (Fig 5.9A, Appendix Table A1), of which 13 major cellular proteins were found with high relative abundance.

In the PT group, 991 proteins were identified, among which differential expression was observed in 689 proteins compared to the control, and the expression of 406 proteins was restored in the PHNP group (Fig 5.9A). Between the PHNP and PT groups, 49 proteins were uniquely expressed (Fig 5.9A).

The scatter plot shows the differential expression of proteins in the PT group of *C. elegans* compared to the CT group of worms (Fig 5.9B). Further, the intracellular

proteins of the PHNP group were compared with the PT and CT groups to identify the differentially expressed proteins involved in apoptosis, electron transport chain, stress response, antioxidant, and ubiquitin-proteasome pathways, which were restored in the PHNP group of worms (Appendix Table A1). The intracellular protein of HNP-treated *C. elegans* was compared with the CT group, of which 297 proteins were uniquely expressed (Fig 5.9C). Proteomics analysis provided evidence of uniquely defined protein-regulated pathways in neuronal growth and development (Table 5.1).

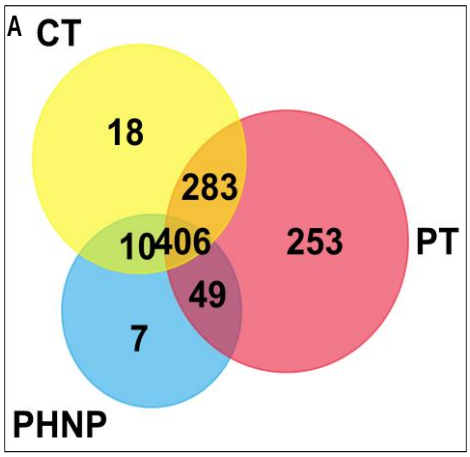

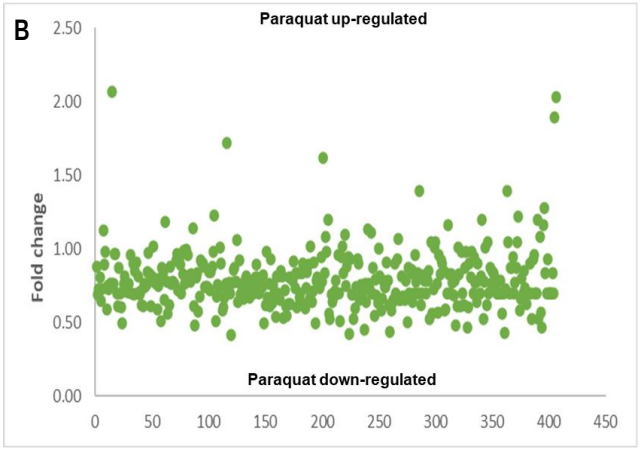

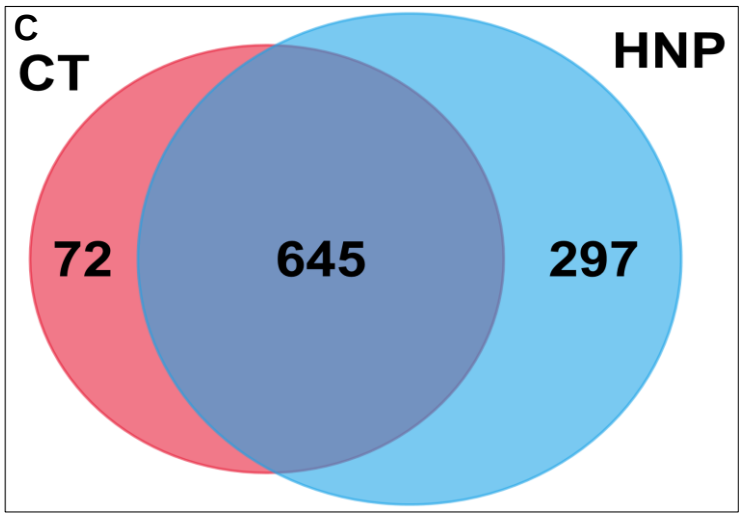

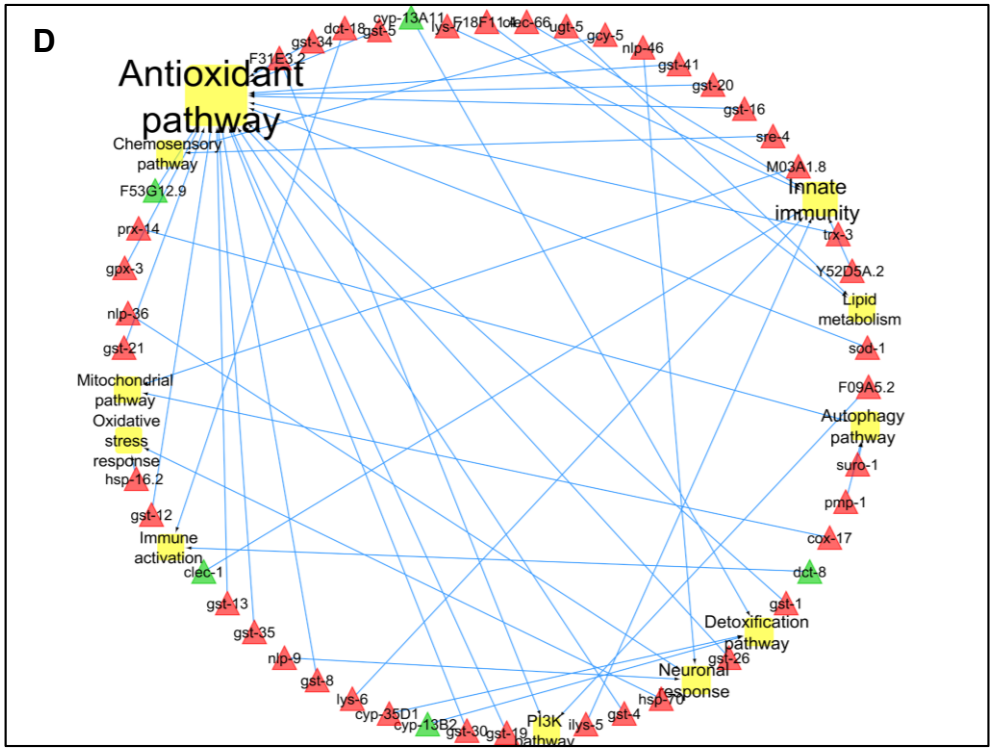

Fig. 5.9 Proteomics analysis to show the expression of common and intracellular proteins among the treated groups of *C. elegans*. (A) Venn diagram showing common intracellular proteins among untreated (control) (CT), PT (PT) treated, and HNP pre-treated followed by PT-treated (PHNP) groups of *C. elegans* determined by LC/MS-MS analysis. (B) Scatter plot showing significantly upregulated (fold change>1.25) and downregulated (fold change <0.80) proteins in PT-treated *C. elegans*. FC: fold-change in expression determined by LC/MS-MS analysis. (C) Venn diagram showing common intracellular proteins among untreated (control) (CT) and only HNP-treated *C. elegans* determined by LC/MS-MS analysis. (D) Molecular network of custom peptide HNP-mediated neuroprotection. The interaction network of peptide HNP-regulated genes/proteins and interlinking pathways as determined by both transcriptomic and proteomic analyses.

Table 5.1. List of the uniquely expressed metabolic pathways in *C. elegans* (N2) treated with HNP compared to untreated (control) *C. elegans*. Quantitative proteomic analyses determined these pathways.

Mapped ID/ Accession number	Pathways name	Proteins
CAEEL|WormBase=WBGene00006460|UniProtKB=Q19775	Activin beta signaling pathway	ppm-1.A
CAEEL|WormBase=WBGene00004307|UniProtKB=Q18246	Heterotrimeric G-protein signaling pathway-Gi alpha and Gs alpha-mediated pathways	rap-1
CAEEL|WormBase=WBGene00004357|UniProtKB=Q22038, CAEEL|WormBase=WBGene00000390|UniProtKB=Q05062	Axon guidance mediated by Slit/Robo	rho-1
CAEEL|WormBase=WBGene00001748|UniProtKB=P48727, CAEEL|WormBase=WBGene00001747|UniProtKB=Q27497	Nicotine pharmacodynamics pathway	gsp-2
CAEEL|WormBase=WBGene00003951|UniProtKB=Q9XUV0, CAEEL|WormBase=WBGene00003949|UniProtKB=Q23237	Proteasome pathway	pbs-5
CAEEL|WormBase=WBGene00021826|UniProtKB=G5EES9	Oxidative stress response	txl-1
CAEEL|WormBase=WBGene00006460|UniProtKB=Q19775	ALP23B_signaling_pathway	ppm-1.A
CAEEL|WormBase=WBGene00019599|UniProtKB=O01590	5-Hydroxytryptamine degradation	acds-10
CAEEL|WormBase=WBGene00004460|UniProtKB=Q04908	Cell cycle	rpn-3
CAEEL|WormBase=WBGene00015337|UniProtKB=P34277	Vitamin C metabolism	gsto-2
CAEEL|WormBase=WBGene00020146|UniProtKB=Q22067	Neurogenesis	maph-1.1,
CAEEL|WormBase=WBGene00001262|UniProtKB=Q09590	Vitamin D metabolism pathway	emb-8
CAEEL|WormBase=WBGene00001914|UniProtKB=K7ZUH9, CAEEL|WormBase=WBGene00003955|UniProtKB=O02115	DNA replication	pcn-1
CAEEL|WormBase=WBGene00006460|UniProtKB=Q19775	MYO_signaling_pathway	ppm-1.A
CAEEL|WormBase=WBGene00008809|UniProtKB=O17806, CAEEL|WormBase=WBGene00010606|UniProtKB=Q9XUT8	Detoxification pathways	cyp-13B2, cyp-13A11
CAEEL|WormBase=WBGene00000547|UniProtKB=Q9N4B1, CAEEL|WormBase=WBGene00000390|UniProtKB=Q05062, CAEEL|WormBase=WBGene00000161|UniProtKB=Q22601, CAEEL|WormBase=WBGene00003171|UniProtKB=P12456, CAEEL|WormBase=WBGene00006537|UniProtKB=P52275,	Huntington disease	clp-7, cdc-42, mec-7, arf-3, gpd-1

CAEEL|WormBase=WBGene00000183|UniProtKB=G5EFK4, CAEEL|WormBase=WBGene00001683|UniProtKB=P04970		
CAEEL|WormBase=WBGene00001683|UniProtKB=P04970	Glycolysis	gpd-1
CAEEL|WormBase=WBGene00020557|UniProtKB=P91455	Adenine and hypoxanthine salvage pathway	T19B4.3
CAEEL|WormBase=WBGene00007175|UniProtKB=Q17499	Nicotinic acetylcholine receptor signalling pathway	B0395.3
CAEEL|WormBase=WBGene00021286|UniProtKB=Q966C7	Pentose phosphate pathway	tald-1
CAEEL|WormBase=WBGene00004357|UniProtKB=Q22038, CAEEL|WormBase=WBGene00000390|UniProtKB=Q05062, CAEEL|WormBase=WBGene00003171|UniProtKB=P12456, CAEEL|WormBase=WBGene00006537|UniProtKB=P52275, CAEEL|WormBase=WBGene00006794|UniProtKB=Q07750	Cytoskeletal regulation by Rho GTPase	rho-1, cdc-42, tbb-2, unc-60
CAEEL|WormBase=WBGene00015064|UniProtKB=Q09438	Purine metabolism	B0228.7
CAEEL|WormBase=WBGene00012149|UniProtKB=G5EDW8	Allantoin degradation	CELE_VF13D12I
CAEEL|WormBase=WBGene00008654|UniProtKB=Q19311, CAEEL|WormBase=WBGene00011064|UniProtKB=Q21774	De novo purine biosynthesis	pfas-1, adsl-1
CAEEL|WormBase=WBGene00011745|UniProtKB=Q94048, CAEEL|WormBase=WBGene00001532|UniProtKB=Q23682, CAEEL|WormBase=WBGene00009306|UniProtKB=P91859	Chemosensory response	sre-4, gcy-5, got-1.2
CAEEL|WormBase=WBGene00017772|UniProtKB=Q22966,	Innate immune response pathways	clec-1
CAEEL|WormBase=WBGene00000390|UniProtKB=Q05062	TGF-beta signalling pathway	cdc-42
CAEEL|WormBase=WBGene00003951|UniProtKB=Q9XUV0, CAEEL|WormBase=WBGene00004505|UniProtKB=O76371, CAEEL|WormBase=WBGene00004501|UniProtKB=Q18787, CAEEL|WormBase=WBGene00004460|UniProtKB=Q04908	Ubiquitin proteasome pathway	pbs-5, rpt-5,
CAEEL|WormBase=WBGene00003747|UniProtKB=H2KZL2 CAEEL|WormBase=WBGene00012145|UniProtKB=Q7YTJ1 CAEEL|WormBase=WBGene00007185|UniProtKB=Q03561	Neuronal process	nlp-36 nlp-9 nlp-46
CAEEL|WormBase=WBGene00006460|UniProtKB=Q19775	GBB_signaling_pathway	ppm-1.A
CAEEL|WormBase=WBGene00012149|UniProtKB=G5EDW8	TCA cycle	CELE_VF13D12I

CAEEL|WormBase=WBGene00007175|UniProtKB=Q17499	Muscarinic acetylcholine receptor 1 and 3 signalling Pathway	B0395.3
CAEEL|WormBase=WBGene00012149|UniProtKB=G5EDW8, CAEEL|WormBase=WBGene00014001|UniProtKB=Q23539, CAEEL|WormBase=WBGene00020139|UniProtKB=P91408	Pyruvate metabolism	pyk-2, eppl-1

5.1.9 Transcriptomic and functional proteomics analyses in unison have elucidated the reversal of PT-induced upregulated and downregulated metabolic pathway genes by pre-treatment of *C. elegans* with neuroprotective peptide

The transcriptomic and quantitative proteomics data explicitly demonstrated the regulation of commonly upregulated and downregulated genes and their intracellular proteins in the PT and HNP groups compared to the CT group of *C. elegans* (N2 strain) The upregulated and downregulated proteins are involved in apoptosis, superoxide removal, lipid and protein metabolism, cellular differentiation, energy metabolism, mitochondrial function, axonal transport, autophagy, and neuronal development pathways in *C. elegans*. The analyses showed that the 15 upregulated (Table 5.2A) and 25 downregulated (Table 5.2B) signaling pathways in PT-treated *C. elegans* (N2 strain) were restored to an average level by the HNP peptide pre-treatment before the addition of PT (Tables 5.2A, B).

The comparative data obtained from transcriptomic, proteomics, and qRT-PCR studies suggest that PT treatment induced upregulation of apoptotic pathways, heterotrimeric G-protein signaling pathway-Gq alpha and Go alpha mediated pathway, ras pathway, p53 pathway, T-cell activation pathway, DA receptor-mediated signaling pathway, and hypoxia response via HIF activation in *C. elegans* (Table 5.2A). In contrast, the downregulation of essential pathways such as antioxidative, detoxification, chemosensory response, EGF receptor signaling, PI3K, ubiquitin-proteasome, neurogenesis, TGF-beta signaling, Axon guidance, FGF signaling, nicotinic acetylcholine receptor signaling, ATP synthesis, TCA cycle, DNA replication, oxidative stress response, glycolysis, and neuronal development was noted post-PT-treatment in *C. elegans* (Table 5.2B). Likewise, the collective analysis of transcriptomic and quantitative proteomics data showed that the HNP group, compared to the CT group, induced the expression of 33 unique signaling pathways (Table 5.1). Moreover, overexpression of the metabolic pathway genes (Table 5.2B) in the PHNP group explicitly validated the enhanced biosynthesis of biomolecules required for neurogenesis and neuroprotection mechanism against PT-induced toxicity in *C. elegans*.

Table 5.2A Transcriptomic and proteomic analyses to show the paraquat-induced upregulated metabolic pathways in wild type N2 strain of *C. elegans*. These pathways were restored to control (normal) level by pre-treatment of worms with neuroprotective custom peptide HNP.

Accession Number	Mapped ID	Metabolic pathway name
P02748	CAEEL|WormBase=WBGene00001149|UniProtKB=P54688, CAEEL|WormBase=WBGene00020831|UniProtKB=O61856	Isoleucine biosynthesis
P00027	CAEEL|WormBase=WBGene00001648|UniProtKB=P51875	Heterotrimeric G-protein signalling pathway-Gq alpha and Go alpha-mediated pathway
P06959	CAEEL|WormBase=WBGene00002183|UniProtKB=Q22100	CCKR signalling map
P00053	CAEEL|WormBase=WBGene00000552|UniProtKB=O16305	T cell activation
P00055	CAEEL|WormBase=WBGene00002190|UniProtKB=P30625	Transcription regulation by bZIP transcription factor
P00059	CAEEL|WormBase=WBGene00002363|UniProtKB=G5EGK8	p53 pathway
P02723	CAEEL|WormBase=WBGene00010083|UniProtKB=O17892	Adenine and hypoxanthine salvage pathway
P05912	CAEEL|WormBase=WBGene00002190|UniProtKB=P30625	Dopamine receptor-mediated signalling pathway
P00006	CAEEL|WormBase=WBGene00017121|UniProtKB=P19974	Apoptosis signalling pathway
P00021	CAEEL|WormBase=WBGene00002363|UniProtKB=G5EGK8	FGF signalling pathway
P00034	CAEEL|WormBase=WBGene00000942|UniProtKB=P19826, CAEEL|WormBase=WBGene00016913|UniProtKB=Q18823	Integrin signalling pathway
P02724	CAEEL|WormBase=WBGene00001149|UniProtKB=P54688	Alanine biosynthesis
P00030	CAEEL|WormBase=WBGene00006922|UniProtKB=Q19213	Hypoxia response via HIF activation
P04393	CAEEL|WormBase=WBGene00016236|UniProtKB=Q18313, CAEEL|WormBase=WBGene00021022|UniProtKB=Q9UA62	Ras Pathway
P02745	CAEEL|WormBase=WBGene00014095|UniProtKB=Q23621	Glutamine glutamate conversion

Table 5.2B Transcriptomic and proteomics analyses to show the paraquat-induced downregulated metabolic pathways in N2 strain *C. elegans*. These pathways were restored to normal (control) levels by pre-treatment of worms with neuroprotective custom peptide HNP.

Accession Number	Mapped ID	Metabolic pathway name
P00012	CAEEL|WormBase=WBGene00008809|UniProtKB=O17806, CAEEL|WormBase=WBGene00010606|UniProtKB=Q9XUT8	Detoxification pathways

P02746	CAEEL|WormBase=WBGene00010645|UniProtKB=G5EBW5, CAEEL|WormBase=WBGene00001337|UniProtKB=Q23315	Heme biosynthesis
P00018	CAEEL|WormBase=WBGene00001515|UniProtKB=Q22720, CAEEL|WormBase=WBGene00004287|UniProtKB=Q94124, CAEEL|WormBase=WBGene00002335|UniProtKB=P22981	EGF receptor signalling pathway
P00019	CAEEL|WormBase=WBGene00013785|UniProtKB=Q9U2T1, CAEEL|WormBase=WBGene00013786|UniProtKB=Q9U2T0	Endothelin signalling pathway
P02771	CAEEL|WormBase=WBGene00016103|UniProtKB=Q18164	Pyrimidine metabolism
P00004	CAEEL|WormBase=WBGene00011745|UniProtKB=Q94048, CAEEL|WormBase=WBGene00001532|UniProtKB=Q23682, CAEEL|WormBase=WBGene00009306|UniProtKB=P91859	Chemosensory response
P00048	CAEEL|WormBase=WBGene00012816|UniProtKB=Q9XWX3, CAEEL|WormBase=WBGene00017183|UniProtKB=O16575, CAEEL|WormBase=WBGene00002335|UniProtKB=P22981	PI3 kinase pathway
P00060	CAEEL|WormBase=WBGene00004466|UniProtKB=O61742, CAEEL|WormBase=WBGene00004503|UniProtKB=P46502, CAEEL|WormBase=WBGene00004465|UniProtKB=Q22253	Ubiquitin proteasome pathway
P00052	CAEEL|WormBase=WBGene00002335|UniProtKB=P22981	TGF-beta signalling pathway
P00049	CAEEL|WormBase=WBGene00020146|UniProtKB=Q22067	Neurogenesis
P00013	CAEEL|WormBase=WBGene00004466|UniProtKB=O61742, CAEEL|WormBase=WBGene00004465|UniProtKB=Q22253	Cell cycle
P00031	CAEEL|WormBase=WBGene00003747|UniProtKB=H2KZL2 CAEEL|WormBase=WBGene00012145|UniProtKB=Q7YTJ1 CAEEL|WormBase=WBGene00007185|UniProtKB=Q03561	Neuronal process
P00016	CAEEL|WormBase=WBGene00003171|UniProtKB=P12456, CAEEL|WormBase=WBGene00004287|UniProtKB=Q94124	Cytoskeletal regulation by Rho GTPase
P00021	CAEEL|WormBase=WBGene00001515|UniProtKB=Q22720, CAEEL|WormBase=WBGene00004287|UniProtKB=Q94124, CAEEL|WormBase=WBGene00006352|UniProtKB=G5EDR3, CAEEL|WormBase=WBGene00002335|UniProtKB=P22981	FGF signalling pathway

P00044	CAEEL|WormBase=WBGene00012437|UniProtKB=Q9XWR0, CAEEL|WormBase=WBGene00002348|UniProtKB=P02567, CAEEL|WormBase=WBGene00003514|UniProtKB=P12845	Nicotinic acetylcholine receptor signalling pathway
P02721	CAEEL|WormBase=WBGene00010419|UniProtKB=Q9XXK1, CAEEL|WormBase=WBGene00000229|UniProtKB=P46561, CAEEL|WormBase=WBGene00022089|UniProtKB=Q95XJ0	ATP synthesis
P00009	CAEEL|WormBase=WBGene00004287|UniProtKB=Q94124	Axon guidance mediated by netrin
P00008	CAEEL|WormBase=WBGene00004287|UniProtKB=Q94124, CAEEL|WormBase=WBGene00004357|UniProtKB=Q22038, CAEEL|WormBase=WBGene00000390|UniProtKB=Q05062	Axon guidance mediated by Slit/Robo
P00045	CAEEL|WormBase=WBGene00000075|UniProtKB=Q94316	Notch signalling pathway
P00007	CAEEL|WormBase=WBGene00016104|UniProtKB=Q18163	Axon guidance mediated by semaphorins
P00051	CAEEL|WormBase=WBGene00018491|UniProtKB=Q9UAV5, CAEEL|WormBase=WBGene00001503|UniProtKB=O17214, CAEEL|WormBase=WBGene00007350|UniProtKB=P53596, CAEEL|WormBase=WBGene00020679|UniProtKB=O61199, CAEEL|WormBase=WBGene00000041|UniProtKB=P34455, CAEEL|WormBase=WBGene00000833|UniProtKB=P34575	TCA cycle
P00017	CAEEL|WormBase=WBGene00008645|UniProtKB=P90829, CAEEL|WormBase=WBGene00004340|UniProtKB=P53016	DNA replication
P00046	CAEEL|WormBase=WBGene00015879|UniProtKB=O45155	Oxidative stress response
P00009	CAEEL|WormBase=WBGene00000390|UniProtKB=Q05062	Axon guidance mediated by netrin
P00024	CAEEL|WormBase=WBGene00011884|UniProtKB=Q27527, CAEEL|WormBase=WBGene00011474|UniProtKB=P54216, CAEEL|WormBase=WBGene00006601|UniProtKB=Q10657, CAEEL|WormBase=WBGene00020185|UniProtKB=P91427	Glycolysis

5.1.10 The molecular network analysis demonstrates the neuroprotective functions of HNP against PT-induced toxicity and neuronal damage

Transcriptomic and proteomic analyses revealed different metabolic pathways involved in HNP-induced protection against PT-induced neuronal damage in N2 strain *C. elegans*. Based on these pieces of information, the molecular interactions, a network of gene expression profiles was constructed (Fig 5.9D). The mapping showed that the interconnected pathways of PT-induced knock-over genes leading to neuronal dysfunction were restored with the HNP pre-treatment in *C. elegans* (Fig 5.9D). In unison, transcriptomic and proteomic studies have identified 15 common upregulated pathways between the PHNP and PT groups of *C. elegans*. The molecular network displayed the snapshot of the genes regulating proteins and their biological functions, modulating the neurogenesis and neuroprotective function of HNP against PT-induced toxicity and neuronal dysfunction (Fig 5.9D, Table 5.1).

An overall neuroprotective mechanism against PT-induced neurotoxicity is proposed in Fig. 5.10.

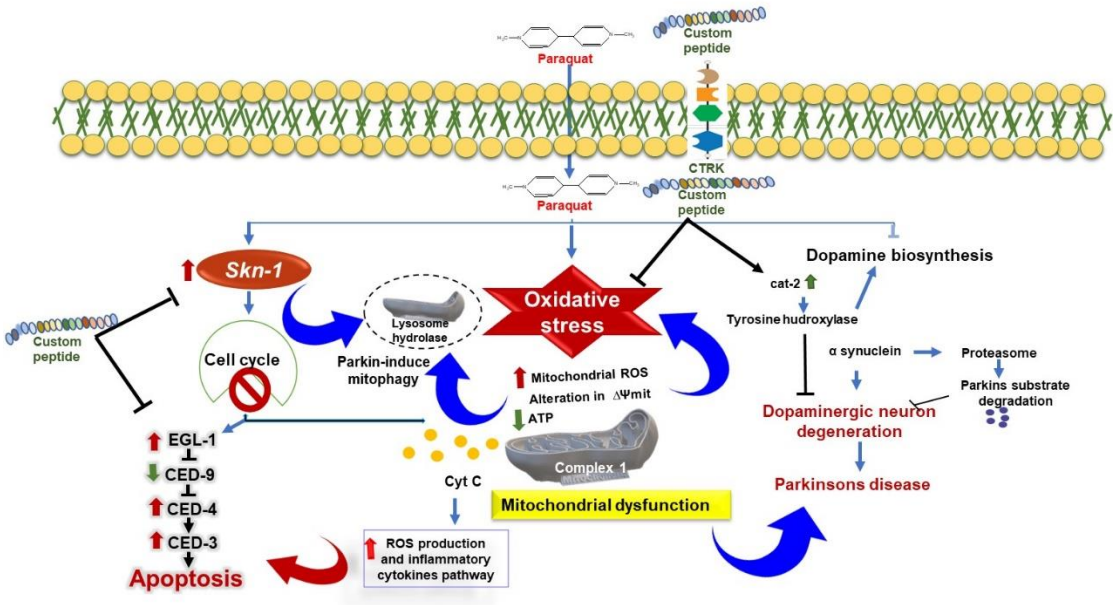

Fig. 5.10 The proposed neuroprotection mechanism pathways of custom peptide mediated protection against PT-induced neurotoxicity in *C. elegans* (N2 strain). DAergic neuronal degeneration and α-synuclein accumulation are two major hallmarks of PD. The PT-induced overexpression of SKN-1 (p38/MAPK) induced response does not protect

DAergic neurons from degeneration, affect cell cycle and trigger the activation of apoptotic pathways. Upregulation of antioxidant enzymes (sods and catalases), accumulation of ROS, and mitochondrial release of cytochrome c upon exposure to neurotoxins such as PT is one of the crucial factors in DAergic neuron degeneration, α-synuclein aggregation, and neuronal death. Custom peptide-pretreatment downregulates SKN-1 pathways, increase stress resistance, ameliorates mitochondrial stress and inhibit activation of apoptotic pathways. Custom peptides-mediated upregulation of the cat-2 gene regulates tyrosine hydroxylase (TH) enzyme expression and restores the PT-induced DA deficiency.

5.1.11 Custom peptides were non-toxic to mice and safe to administer

Custom peptides (TNP and HNP at the ratio 1:1, 10.0 mg/kg) were non-toxic to mice and did not show behavioral changes or adverse effects in treated mice. The serum profiles viz. serum glutamic oxaloacetic transaminase (SGOT), alkaline phosphatase (ALKP), serum glutamic pyruvic transaminase (SGPT), BUN (blood urea nitrogen), glucose content, creatinine, cholesterol, bilirubin and albumin of the custom peptide-treated mice (24 h post-treatment) did not show any significant ($p \geq 0.05$) deviation compared to the control (1X PBS treated) group of mice (Table 5.3). A minor increase in glucose level was measured in the blood of the treated mice compared to control mice, but it was within the normal range of blood glucose in mice (Table 5.3). The acute toxicity studies in mice models showed that the peptide is devoid of toxicity in mice at a dose that is 100 times higher than its therapeutic dose determined in *C. elegans*. Moreover, microscopic examination of the brain, heart, kidney, liver, lung, ovary, and testis of the custom peptide (HNP)-treated mice showed no morphological alterations (Fig 5.11). However, HNP treatment significantly ($p \leq 0.05$) reduced the production of pro-inflammatory cytokines viz. TNF-α, IL-6, IL-1β, compared to the control group of mice (Fig 5.12).

Table 5.3 Some biochemical properties of serum of control and custom peptides (TNP and HNP; 1:1)-treated (10 mg/kg) mice after 24 hours of *i.v.* injection. Values are mean ± SD of 6 mice. There was no significant difference in values ($p \geq 0.05$) between control and custom peptides-treated groups of mice.

	Values		
Parameters (Unit)	**Control**	**Custom peptides-treated**	**Normal Range**
Glucose (mg/dL)	101.10 ± 1.27	160.0 ± 1.50	60-133
Billirubin (Direct) (mg/dL)	0.03 ± 0.00	0.08 ± 0.00	0.01-0.4
Billirubin (Total) (mg/dL)	0.05 ± 0.00	0.1 ± 0.00	0.05-0.9
BUN (mg/dL)	8 ± 0.05	10 ± 0.10	2-71
Creatinine(mg/dL)	0.18 ± 0.20	0.17 ± 0.20	0.1-1.8
Albumin (mg/dL)	1.98 ± 0.03	2.1 ± 0.05	2.6-5.4
ALKP(U/L)	81.85 ± 1.63	132 ± 1.70	16-200
SGPT(U/L)	33 ± 0.78	36 ± 0.70	22-133
SGOT(U/L)	62 ± 1.10	64 ± 1.13	46-221
Cholesterol (mg/dL)	66 ± 2.5	70 ± 3.0	34-173

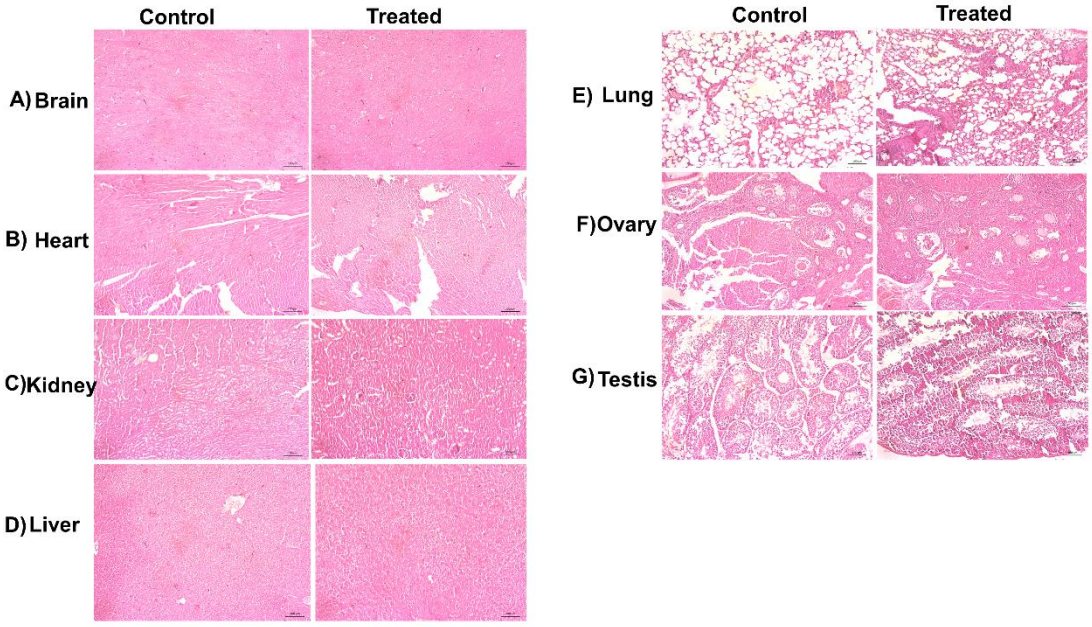

Fig 5.11 The effect of the custom peptides (TNP: HNP:: 1:1) treatment on histological changes in the tissues of Swiss albino mice. The H and E staining was employed to observe any morphological changes in the tissues compared to those of the control

(untreated). Light microscopic observation of (A) Brain, (B) Heart, (C) Kidney, (D) Liver, (E) Lung, (F) Ovary, and (G) Testis for control and treated groups. Bar-100µM.

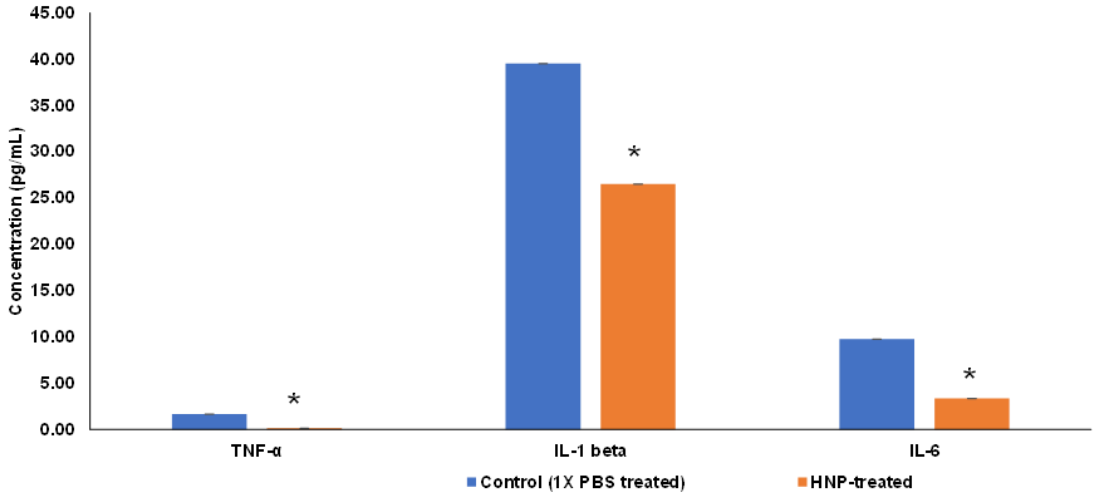

Fig 5.12 Determination of the concentration of pro-inflammatory cytokines in control (1X PBS treated)/ custom peptides-treated (10 mg/kg) group of mice plasma by Quantikine HS ELISA Kit. * A significant difference between control (1X PBS-treated) and custom peptide (TNP:HNP)-treated *C. elegans* ($p < 0.05$). Values are means ± SD of triplicate determinations.

5.2 Discussion

In recent years, the characterization of novel neurotrophic peptides has gained more focus in clinical trials against different NDs [7-11]. Neurotrophic peptides have several advantages over other neurotrophic drugs, such as improved neuroprotective effect, synaptic and neuronal plasticity, neurogenesis, better pharmacokinetics than the parent neurotrophin, and easy penetration [12,13].

Our previous study has demonstrated the exclusive binding of TNP and HNP to the TrkA receptor of PC-12 cells to induce neuritogenesis [14]; however, *C. elegans* possesses a simple nervous system and lacks Trk receptors [15]. Therefore, we were puzzled to understand the region of binding and mechanism of neuroprotective activity of custom peptides and mouse-NGF in *C. elegans*. To solve this issue, we investigated the presence of TrkA receptor homolog in the *C. elegans*. The presence of TrkA receptor homolog CAM-1 receptor in *C. elegans* was discovered by BLAST search.

Further *in silico* studies validated the binding of custom peptides and mouse-NGF to the CAM-1 receptor. The CAM-1 in *C. elegans* is a less functionally explored protein receptor. However, some reports suggest that CAM-1 is involved in essential functions, viz., the regulation of asymmetric division of V cells (seam cells), CA/CP neuroblast, and axon outgrowth [16,17] and the positioning of the nerve ring [18]. Further, the CAM-1 receptor is also responsible for the negative regulation of developmental neurite pruning of AIM neurons [19]. Moreover, Entries in the Reactome pathway browser database [1] demonstrated that the CAM-1 receptor is an essential component in the MAPK signaling pathway by playing multiple roles, such as the regulation and development of axons [16,17] and the positioning of the nerve ring [18].

Therefore, the CAM-1 receptor as a confirmed binding site for the custom peptides in this study was further validated by insignificant binding of FITC-custom peptides in the CAM-1 mutant strain of *C. elegans* at its nerve ring region. However, FITC-conjugated custom peptides showed binding to *C. elegans* at its nerve ring adjacent to the pharynx, which covers complex circuitry leading to most aspects of behaviors, such as chemosensation, locomotion, learning, memory, etc. [20]. The nerve ring of *C. elegans* adjacent to the pharynx functions similarly to a "brain' and most sensory neurons have endings organized around the mouth [20].

PD is associated with multiple motor and non-motor symptoms developed due to elevated oxidative stress leading to mitochondrial membrane damage, which triggers DAergic neuron degeneration [21]. A plethora of reports support that oxidative stress is one of the essential factors associated with the progression of NDs such as PD, and evidence has been presented to show that antioxidant activity may prevent ND [22,23]. We have demonstrated the *in vitro* antioxidant properties of the TNP and HNP by their free radical scavenging activity [2]. Therefore, TNP and HNP *in vivo* conditions also prolong the lifespan by decreasing the oxidative stress in worms [24,25]. Antioxidants such as vitamin C and quercetin demonstrated neuroprotection properties in several *in vitro* and *in vivo* models of NDs viz. AD, PD, and Huntington's Disease (HD) [26-28]. Therefore, we considered quercetin and vitamin C a positive control for this study.

Since ASH sensory neurons of *C. elegans* play a pivotal role in the sensory response to aversive stimuli, PT treatment induces defective chemotaxis behavior in

worms due to the loss of ASH neuronal function [5]. Therefore, the chemotaxis assay was performed in *C. elegans* to demonstrate the possibility of restoration of PT-induced chemotaxis dysfunction by pre-treatment with custom peptides. The pre-treatment of *C. elegans* with custom peptides before PT treatment has shown a superior protective effect by restoring the PT-induced chemotaxis defect and survivability, which may be correlated to the fact that these peptides bind to the same region (nerve ring adjacent to the pharynx) where PT binds to induce neurodegeneration in *C. elegans*. Therefore, post-administration of peptides after PT treatment, minimal protection was observed against PT-induced neurodegeneration when they already bind to neurons. Further, peptides' neuroprotective and neurotrophic effects were validated from the transcriptomic and proteomic analysis data. Both unambiguously showed that the proteins responsible for chemosensory behavior, viz. sre-4, gcy-5, and got-1.2 were downregulated by PT, resulting in the loss of memory of *C. elegans*. In sharp contrast, pre-treatment with custom peptides upregulated these genes to increase the cellular proteins to an average level (untreated control worms).

The increased ROS content observed in the neurons of PD patients and PD-like model organisms triggers cellular damage and apoptosis [25,29,30]. Therefore, antioxidant compounds, for example, quercetin, curcumin, naringin, metformin, bacosides, hydralazine, and vitamin C, have found significant therapeutic potential to treat PT-induced toxicity [31-34]. For preventing cellular damage and neurodegeneration in a non-autonomous fashion, mitochondrial dysfunction triggers the upregulation of many stress response pathways, such as p38/MAPK innate immune pathways [35]. HNP and TNP [50 µg/mL; 41.6 µM (TNP) and 35.7 µM (HNP)] pre-treatment for 2 h demonstrated appreciable potency to reduce the PT-mediated increase in cellular ROS level and mitochondrial membrane depolarization, subsequently enhancing survival rates in PT-treated *C. elegans*. Vitamin C pre-treatment for 24 h significantly attenuated the PT-induced ROS production but did not restore mitochondrial membrane depolarization at a concentration (100 µg/mL) two times higher than the concentration of custom peptides. Further, vitamin C could not offer protection against PT-induced neurotoxicity, thus implying that PT-induced neuronal damage may not be protected only by the antioxidant property of the peptides, which rationalizes the therapeutic potency of custom peptides under study.

In response to oxidative stress, the *skn-1* gene translocates and accumulates at the intestinal nuclei and induces transcription of genes such as SODs (*sod-1* and *sod-3*), catalases (*cat-1, cat-2 ,* and *cat3*), thioredoxin-1 (*trx-1*), GSTs (*gst-4, gst-6* and *gst-10*), and heat-shock proteins HSPs (*hsp-16.1* and *hsp-16.2*) involved in phase 2 detoxification [36]. Accordingly, the MAPK genes *sek-1, pmk-1,* and *skn-1* were upregulated in *C. elegans* post-PT exposure. However, the qRT-PCR results have shown the overexpression of downstream genes of activated p38/MAPK pathways such as '*skn-1'* that regulates various detoxification processes (*sod, cat, trx,* and *gst* series) and heat-shock proteins (HSPs) genes essential to abolish enhanced ROS production leading to cellular damage [35,37]. The expression level of SODs and other associated genes is low under normal conditions [37,38]. However, acute exposure to PT induces higher expression of such genes in mitochondria to withstand oxidative stress. The PT-mediated over-expression of HSPs prevents the protein from misfolding due to changes in the cellular redox state [39]. The qRT-PCR result highlighted the significant downregulation of stress-related genes in custom peptide-treated wild-type N2 worms compared to the PT treatment, probably due to the enhanced transcription initiation or mRNA stability. Downregulation of these genes upon custom peptide pre-treatment is correlated with reduced oxidative stress and increased stress resistance in *C. elegans,* which concludes the antioxidant and neuroprotective potential of TNP and HNP.

DAergic neurons are vulnerable to PT-induced oxidative stress due to ROS generation, a principal neuronal death regulator [40]. DAergic neuronal degeneration and α-synuclein accumulation are two major hallmarks of PD [41]. The PT-induced overexpression of SKN-1 (p38/MAPK) induced response does not protect DAergic neurons from degeneration [35]. Upregulation of antioxidant enzymes (sods and catalases) and accumulation of ROS upon exposure to neurotoxins such as PT is one of the crucial factors in DAergic neuron degeneration and α-synuclein aggregation [42]. Custom peptides-mediated upregulation of the *cat-2* gene regulates tyrosine hydroxylase (TH) enzyme expression and restores the PT-induced DA deficiency [43].

The neurotransmitter DA availability to the striatum (brain structure) is essential for motor response and memory functions [44,45]. DA deficiency is another hallmark of PD, resulting in DAergic cell death and α-synuclein deposition [45,46]. The

neuroprotective activity of custom peptides against PT-induced chemotaxis behavior defects, DAergic neurodegeneration, α-synuclein accumulation, and reduced life span may be correlated to their antioxidant and antiapoptotic properties [40]. However, vitamin C was ineffective in restoring chemotaxis behavior, DAergic neurodegeneration, and α-synuclein accumulation induced by the acute exposure of PT in C. elegans, so reinforcing antioxidation may not be the only property to offer protection against PT-induced neurodegeneration [2].

The custom peptide HNP surpassed TNP in preventing PT-induced toxicity; subsequently, it was selected for further studies. The cumulative data generated from *in silico,*qRT-PCR, transcriptomic, and proteomics analysis have unambiguously demonstrated that HNP pre-treatment resulted in the downregulation of PT-induced upregulated pro-apoptotic (cytochrome C, CED-4, and CED-3) genes expression. In contrast, it upregulated the expression of antiapoptotic genes (CED-9) in PT-treated *C. elegans,* thereby enhancing the survival rate of worms.

The transcriptomic and quantitative proteomic analyses have identified the molecular network of signaling pathways through which the peptide HNP blocked the PT-induced neurotoxicity in *C. elegans*. The findings aided that HNP pre-treatment restored the PT-induced altered genes and protein functions such as antioxidant pathways, mitochondrial stress response pathways, energy metabolism pathways, lipid and protein metabolism pathways, and programmed cell death in *C. elegans*.

The custom peptide also restored altered pathways induced by the PT treatment in the *C. elegans* PD model (N2 strain). PT causes its toxic effect by downregulating most of the antioxidant genes (sod, trx, gst), mitochondrial stress resistance gene (txl-1, cox-4), detoxification genes (cyp-13B2, cyp-13A11), TCA cycle (CELE_VF13D12L), genes involved in chemosensory response (sre-4, gcy-5, got-1.2), neurogenesis (maph-1.1), neuronal development (nlp-36, nlp-9, nlp-46) and upregulated apoptotic genes (cyt C, egl-1), MAPK genes involved in innate immune response (skn-1), and some of the stress response genes (hsp10) in *C. elegans*, which were counteracted by custom peptide (HNP) pre-treatment.

In a nutshell, the PT group of worms exhibited the maximal variation in differential gene expression compared with the CT group of *C. elegans.* In contrast, the

custom peptides pre-treatment group showed a minimum variance compared to the CT group, signifying normalization or restoration of altered genes/proteins dynamics. This study highlights the therapeutic importance of custom peptides for attenuating neurodegeneration.

Using the tested custom peptides as a drug prototype exclusively depends upon their non-toxic nature in preclinical studies. Further, it has no detrimental effect on the biochemical parameters of blood parameters and vital organs, suggesting the safety of the peptides for the development of drug prototypes. In this study, the therapeutic dose of the custom peptide was first determined in *C. elegans*, a small organism used as an initial model. When we tested the peptide in mice, we administered a dose that was 100 times higher than the effective therapeutic dose used in *C. elegans*. This was done to assess whether the peptide would cause any toxicity at much higher concentrations. Furthermore, the reduced concentration of inflammatory mediators (TNF-α, IL-6, IL-1β) in the HNP-treated mice, compared to control (1X PBS-treated) mice, diminished the risk of inflammatory response post-treatment with peptides. One of our future goals is to assess the neuroprotective effect and pharmacokinetics and pharmacodynamics properties of the custom peptides in rodent models. Also, transcriptomics and proteomics studies have provided a broad insight into general pathways that are up or downregulated by custom peptides to protect against PT-induced neurodegeneration. Further in-depth mechanistic insights of custom peptides are warranted.

Bibliography

[1] Fabregat, A., Sidiropoulos, K., Viteri, G., Marin-Garcia, P., Ping, P., Stein, L., D'Eustachio, P., and Hermjakob, H. Reactome diagram viewer: data structures and strategies to boost performance. *Bioinformatics*, 34(7): 1208-1214, 2018.

[2] Madhubala, D., Patra, A., Islam, T., Saikia, K., Khan, M. R., Ahmed, S. A., Borah, J. C., and Mukherjee, A. K. Snake venom nerve growth factor-inspired designing of novel peptide therapeutics for the prevention of paraquat-induced apoptosis, neurodegeneration, and alteration of metabolic pathway genes in the rat pheochromocytoma PC-12 cell. *Free Radical Biology Medicine*, 197: 23-45, 2023.

[3] Salahudeen, M. S. and Nishtala, P. S. An overview of pharmacodynamic modelling, ligand-binding approach and its application in clinical practice. *Saudi Pharmaceutical Journal*, 25(2): 165-175, 2017.

[4] Ray, A., Martinez, B., Berkowitz, L., Caldwell, G., and Caldwell, K. Mitochondrial dysfunction, oxidative stress, and neurodegeneration elicited by a bacterial metabolite in a *C. elegans* Parkinson's model. *Cell death disease*, 5(1): e984-e984, 2014.

[5] Dilberger, B., Baumanns, S., Schmitt, F., Schmiedl, T., Hardt, M., Wenzel, U., and Eckert, G. P. Mitochondrial oxidative stress impairs energy metabolism and reduces stress resistance and longevity of C. elegans. *Oxidative medicine cellular longevity*, 2019: 1-14, 2019.

[6] Zhu, Q., Qu, Y., Zhou, X.-G., Chen, J.-N., Luo, H.-R., and Wu, G.-S. A dihydroflavonoid naringin extends the lifespan of *C. elegans* and delays the progression of aging-related diseases in PD/AD models via DAF-16. *Oxidative medicine cellular longevity*, 2020: 1-14, 2020.

[7] Kim, S., Nam, H. Y., Lee, J., and Seo, J. Mitochondrion-targeting peptides and peptidomimetics: recent progress and design principles. *Biochemistry*, 59(3): 270-284, 2019.

[8] Ben-Shushan, S. and Miller, Y. Neuropeptides: Roles and activities as metal chelators in neurodegenerative diseases. *The Journal of Physical Chemistry B*, 125(11): 2796-2811, 2021.

[9] Lee, K. and Mylonakis, E. An intestine-derived neuropeptide controls avoidance behavior in *Caenorhabditis elegans*. *Cell reports*, 20(10): 2501-2512, 2017.

[10] Wongchai, K., Schlotterer, A., Lin, J., Humpert, P., Klein, T., Hammes, H.-P., and Morcos, M. Protective effects of liraglutide and linagliptin in *C. elegans* as a new model for glucose-induced neurodegeneration. *Hormone Metabolic Research*, 48(01): 70-75, 2016.

[11] Swindell, W. R., Bojanowski, K., Kindy, M. S., Chau, R. M., and Ko, D. GM604 regulates developmental neurogenesis pathways and the expression of genes associated with amyotrophic lateral sclerosis. *Translational neurodegeneration*, 7(1): 1-24, 2018.

[12] Longo, F. M. and Massa, S. M. Small-molecule modulation of neurotrophin receptors: a strategy for the treatment of neurological disease. *Nature reviews Drug discovery*, 12(7): 507-525, 2013.

[13] Gudasheva, T. A., Povarnina, P., Tarasiuk, A. V., and Seredenin, S. B. The low molecular weight brain-derived neurotrophic factor mimetics with antidepressant-like activity. *Current Pharmaceutical Design*, 25(6): 729-737, 2019.

[14] Patapoutian, A. and Reichardt, L. F. Trk receptors: mediators of neurotrophin action. *Current opinion in neurobiology*, 11(3): 272-280, 2001.

[15] Jaaro, H., Beck, G., Conticello, S. G., and Fainzilber, M. Evolving better brains: a need for neurotrophins? *Trends in neurosciences*, 24(2): 79-85, 2001.

[16] Kim, C. and Forrester, W. C. Functional analysis of the domains of the *C. elegans* Ror receptor tyrosine kinase CAM-1. *Developmental Biology*, 264(2): 376-390, 2003.

[17] Forrester, W. C., Dell, M., Perens, E., and Garriga, G. A C. elegans Ror receptor tyrosine kinase regulates cell motility and asymmetric cell division. *Nature*, 400(6747): 881-885, 1999.

[18] Kennerdell, J. R., Fetter, R. D., and Bargmann, C. I. Wnt-Ror signaling to SIA and SIB neurons directs anterior axon guidance and nerve ring placement in C. elegans. *Development*, 136(22): 3801-3810, 2009.

[19] Hayashi, Y., Hirotsu, T., Iwata, R., Kage-Nakadai, E., Kunitomo, H., Ishihara, T., Iino, Y., and Kubo, T. A trophic role for Wnt-Ror kinase signaling during developmental pruning in Caenorhabditis elegans. *Nature Neuroscience*, 12(8): 981-987, 2009.

[20] Ware, R. W., Clark, D., Crossland, K., and Russell, R. L. The nerve ring of the nematode *Caenorhabditis elegans*: sensory input and motor output. *Journal of Comparative Neurology*, 162(1): 71-110, 1975.

[21] Percário, S., da Silva Barbosa, A., Varela, E. L. P., Gomes, A. R. Q., Ferreira, M. E. S., de Nazaré Araújo Moreira, T., and Dolabela, M. F. Oxidative stress in parkinson's disease: Potential benefits of antioxidant supplementation. *Oxidative medicine cellular longevity*, 2020: 1-23, 2020.

[22] Zhou, C., Huang, Y., and Przedborski, S. Oxidative stress in Parkinson's disease: a mechanism of pathogenic and therapeutic significance. *Annals of the new York Academy of Sciences*, 1147(1): 93-104, 2008.

[23] Shi, D., Yang, J., Jiang, Y., Wen, L., Wang, Z., and Yang, B. The antioxidant activity and neuroprotective mechanism of isoliquiritigenin. *Free Radical Biology Medicine*, 152: 207-215, 2020.

[24] Carocho, M., Ferreira, I. C., Morales, P., and Soković, M. Vol. 2020 1-23 (Oxidative Medicine Cellular Longevity, 2019).

[25] Kvetkina, A., Pislyagin, E., Menchinskaya, E., Yurchenko, E., Kalina, R., Kozlovskiy, S., Kaluzhskiy, L., Menshov, A., Kim, N., and Peigneur, S. Kunitz-Type Peptides from Sea Anemones Protect Neuronal Cells against Parkinson's Disease Inductors via Inhibition of ROS Production and ATP-Induced P2X7 Receptor Activation. *International journal of molecular sciences*, 23(9): 5115, 2022.

[26] Rishitha, N. and Muthuraman, A. Therapeutic evaluation of solid lipid nanoparticle of quercetin in pentylenetetrazole induced cognitive impairment of zebrafish. *Life Sciences*, 199: 80-87, 2018.

[27] Grewal, A. K., Singh, T. G., Sharma, D., Sharma, V., Singh, M., Rahman, M. H., Najda, A., Walasek-Janusz, M., Kamel, M., and Albadrani, G. Mechanistic insights and perspectives involved in neuroprotective action of quercetin. *Biomedicine & Pharmacotherapy*, 140: 111729, 2021.

[28] El-Horany, H. E., El-latif, R. N. A., ElBatsh, M. M., and Emam, M. N. Ameliorative effect of quercetin on neurochemical and behavioral deficits in rotenone rat model of Parkinson's disease: modulating autophagy (quercetin on experimental Parkinson's disease). *Journal of Biochemical Molecular Toxicology*, 30(7): 360-369, 2016.

[29] Cooper, J. F., Dues, D. J., Spielbauer, K. K., Machiela, E., Senchuk, M. M., and Van Raamsdonk, J. M. Delaying aging is neuroprotective in Parkinson's disease: a genetic analysis in C. elegans models. *NPJ Parkinson's disease*, 1(1): 1-12, 2015.

[30] Zhang, J., Shi, R., Li, H., Xiang, Y., Xiao, L., Hu, M., Ma, F., Ma, C. W., and Huang, Z. Antioxidant and neuroprotective effects of Dictyophora indusiata polysaccharide in *Caenorhabditis elegans*. *Journal of ethnopharmacology*, 192: 413-422, 2016.

[31] Hou, R. R., Chen, J. Z., Chen, H., Kang, X. G., Li, M. G., and Wang, B. R. Neuroprotective effects of (-)-epigallocatechin-3-gallate (EGCG) on paraquat-induced apoptosis in PC12 cells. *Cell Biol Int*, 32(1): 22-30, 2008. 10.1016/j.cellbi.2007.08.007

[32] Blanco-Ayala, T., Andérica-Romero, A., and Pedraza-Chaverri, J. New insights into antioxidant strategies against paraquat toxicity. *Free radical research*, 48(6): 623-640, 2014.

[33] Jia, W., Su, Q., Cheng, Q., Peng, Q., Qiao, A., Luo, X., Zhang, J., and Wang, Y. Neuroprotective Effects of Palmatine via the Enhancement of Antioxidant Defense and Small Heat Shock Protein Expression in Aβ-Transgenic *Caenorhabditis elegans*. *Oxidative medicine cellular longevity*, 2021:9966223, 2021.

[34] Dehghan, E., Zhang, Y., Saremi, B., Yadavali, S., Hakimi, A., Dehghani, M., Goodarzi, M., Tu, X., Robertson, S., and Lin, R. Hydralazine induces stress resistance and extends *C. elegans* lifespan by activating the NRF2/SKN-1 signalling pathway. *Nature communications*, 8(1): 1-14, 2017.

[35] Chikka, M. R., Anbalagan, C., Dvorak, K., Dombeck, K., and Prahlad, V. The mitochondria-regulated immune pathway activated in the *C. elegans* intestine is neuroprotective. *Cell reports*, 16(9): 2399-2414, 2016.

[36] Ma, X., Li, J., Cui, X., Li, F., and Wang, Z. Dietary supplementation with peptides from sesame cake protect *Caenorhabditis elegans* from polyglutamine-induced toxicity. *Journal of Functional Foods*, 54: 199-210, 2019.

[37] Yee, C., Yang, W., and Hekimi, S. The intrinsic apoptosis pathway mediates the pro-longevity response to mitochondrial ROS in *C. elegans*. *Cell*, 157(4): 897-909, 2014.

[38] Kumar, A., Joishy, T., Das, S., Kalita, M. C., Mukherjee, A. K., and Khan, M. R. A potential probiotic *Lactobacillus plantarum* JBC5 improves longevity and healthy aging by modulating antioxidative, innate immunity and serotonin-signaling pathways in *Caenorhabditis elegans*. *Antioxidants*, 11(2): 268, 2022.

[39] Taylor, S. K., Minhas, M. H., Tong, J., Selvaganapathy, P. R., Mishra, R. K., and Gupta, B. P. *C. elegans* electrotaxis behavior is modulated by heat shock response and unfolded protein response signaling pathways. *Scientific reports*, 11(1): 1-17, 2021.

[40] Gonzalez-Hunt, C. P., Leung, M. C., Bodhicharla, R. K., McKeever, M. G., Arrant, A. E., Margillo, K. M., Ryde, I. T., Cyr, D. D., Kosmaczewski, S. G., and Hammarlund, M. Exposure to mitochondrial genotoxins and dopaminergic neurodegeneration in Caenorhabditis elegans. *PloS one*, 9(12): e114459, 2014.

[41] Oliveira, L. M., Gasser, T., Edwards, R., Zweckstetter, M., Melki, R., Stefanis, L., Lashuel, H. A., Sulzer, D., Vekrellis, K., and Halliday, G. M. Alpha-synuclein research: Defining strategic moves in the battle against Parkinson's disease. *NPJ Parkinson's disease*, 7(1): 65, 2021.

[42] Bové, J. and Perier, C. Neurotoxin-based models of Parkinson's disease. *Neuroscience*, 211: 51-76, 2012.

[43] Saewanee, N., Praputpittaya, T., Malaiwong, N., Chalorak, P., and Meemon, K. Neuroprotective effect of metformin on dopaminergic neurodegeneration and α-synuclein aggregation in *C. elegans* model of Parkinson's disease. *Neuroscience Research*, 162: 13-21, 2021.

[44] Graybiel, A. M., Aosaki, T., Flaherty, A. W., and Kimura, M. The basal ganglia and adaptive motor control. *Science*, 265(5180): 1826-1831, 1994.

[45] McKinley, J. W., Shi, Z., Kawikova, I., Hur, M., Bamford, I. J., Devi, S. P. S., Vahedipour, A., Darvas, M., and Bamford, N. S. Dopamine deficiency reduces striatal cholinergic interneuron function in models of Parkinson's disease. *Neuron*, 103(6): 1056-1072. e1056, 2019.

[46] Jankovic, J. and Poewe, W. Therapies in Parkinson's disease. *Current opinion in neurology*, 25(4): 433-447, 2012.